# Shebandowan greenstone belt, western Superior Province: U-Pb ages, tectonic implications, and correlations

**F. Corfu*** *Jack Satterly Laboratory, Royal Ontario Museum, 100 Queen's Park, Toronto, Ontario M5S 2C6, Canada*

**G. M. Stott** *Ontario Geological Survey, Willet Green Miller Centre, 933 Ramsey Lake, Road, Sudbury, Ontario P3E 6B5, Canada*

## ABSTRACT

**The Shebandowan greenstone belt of the western Wawa Subprovince consists of successions of volcanic and sedimentary rocks impinging onto the metasedimentary Quetico Subprovince to the north and cored by a batholithic complex to the south. U-Pb geochronology using mainly zircon and titanite demonstrates a relatively rapid accretion of the greenstone belt in the late Archean. The oldest ages were obtained for 2750 Ma tonalitic gneiss and sporadic 2830–2750 Ma detrital or xenocrystic zircons. A major phase of greenstone belt construction at 2720 Ma formed ultramafic to felsic volcanic rocks and peridotitic, gabbroic, and anorthositic bodies, probably in an extensional arc–backarc setting. These units are laterally correlative with volcanogenic massive sulfide-bearing assemblages in the central Wawa Subprovince and probably with similar successions in northern Minnesota. The second major stage of felsic volcanism and plutonism at about 2695 Ma was associated with $D_1$ compression causing thrusting, imbrication, and sedimentation. This was succeeded by the deposition of an unconformable sequence of calc-alkalic to alkalic volcanic and sedimentary rocks and emplacement of tonalitic to syenitic plutons at about 2690 Ma. Transpressive deformation ($D_2$), constrained between 2685 and 2680 Ma, caused the development of locally penetrative structures and deposition of clastic sedimentary packages. The emplacement of plutons at 2683–2680 Ma concluded the evolution of the greenstone belt. Titanite (and rutile) yield ages in the same range as zircon, showing that the greenstone belt was situated at high crustal levels by 2680 Ma and escaped the younger and intense deformational-metamorphic events recorded in greenstone belts farther east in the central Wawa Subprovince as well as in the immediately adjacent migmatitic Quetico Subprovince to the north.**

*E-mail: fernando@rom.on.ca.

## INTRODUCTION

The Wawa Subprovince in the southwestern Superior Province comprises a number of Archean greenstone belts, separated by granitoid terranes, and locally disrupted or covered by Proterozoic igneous rocks and sedimentary sequences of the Lake Superior region. The greenstone belts share some common geological characteristics but also display distinct structural and metamorphic records and mineral deposit types. Unraveling the geological histories of each area is important in order to assess metallogenetic correlations across the Subprovince, reconstruct the orogenic evolution of the Superior Province, and understand the overall mechanisms of Archean crustal development.

This geochronological study is focused on the Shebandowan greenstone belt, parts of the neighboring Saganagons greenstone belt, and the surrounding batholiths (Fig. 1). We address questions concerning the early magmatic accretion and stratigraphic correlations of the Shebandowan greenstone belt and examine the relations between felsic volcanic rocks and the abundant mafic-ultramafic complexes characteristic of the belt and their relations to similar units elsewhere in the Wawa Subprovince. We also address the orogenic history as revealed by mutual relationships between structures, sedimentary basins, "Timiskaming-type" volcanic assemblages, and syntectonic to late tectonic plutonic suites, and compare the timing of these events with those recorded elsewhere in the Superior Province.

## GEOLOGICAL SETTING AND SAMPLE CHARACTERISTICS

### General Features

The Shebandowan area comprises three major geological domains: (1) the Shebandowan greenstone belt in the north to northeast; (2) the Saganagons greenstone belt in the southwest; and (3) the Northern Light–Perching Gull Lakes batholithic complex in the south (Fig. 1). Although disrupted by faults and granitoid intrusions, the two greenstone belts appear to be part of a single succession of supracrustal rocks. The Shebandowan greenstone belt impinges onto the metasedimentary Quetico Subprovince to the north and in the southwest it extends toward the Soudan and Newton belts of the Vermilion district of northern Minnesota (Williams et al., 1991). The southeastern part of the region is overlain by Proterozoic strata of the Animikie basin and by Keweenawan volcanic and gabbroic complexes of the Midcontinent rift.

Supracrustal rocks of the Shebandowan greenstone belt define a steeply north-dipping to subvertical oroclinal arc. They have traditionally been subdivided into (1) an older "Keewatin-type" succession of ultramafic to felsic volcanic rocks and associated mafic-ultramafic complexes, and (2) a younger, unconformably overlying "Timiskaming-type" assemblage of clastic sedimentary rocks and calc-alkalic to alkalic volcanic units (Shegelski, 1980). On the basis of the information from early regional mapping the "Keewatin-type" successions were tentatively subdivided into discrete assemblages by Williams et al. (1991): a predominantly north-younging Burchell assemblage in the northern part of the Shebandowan greenstone belt; a south-younging Greenwater assemblage in the southern part of the Shebandowan greenstone belt; and the north-younging Saganagons assem-

*GSA Bulletin*; November 1998; v. 110; no. 11; p. 1467–1484; 9 figures; 1 table.

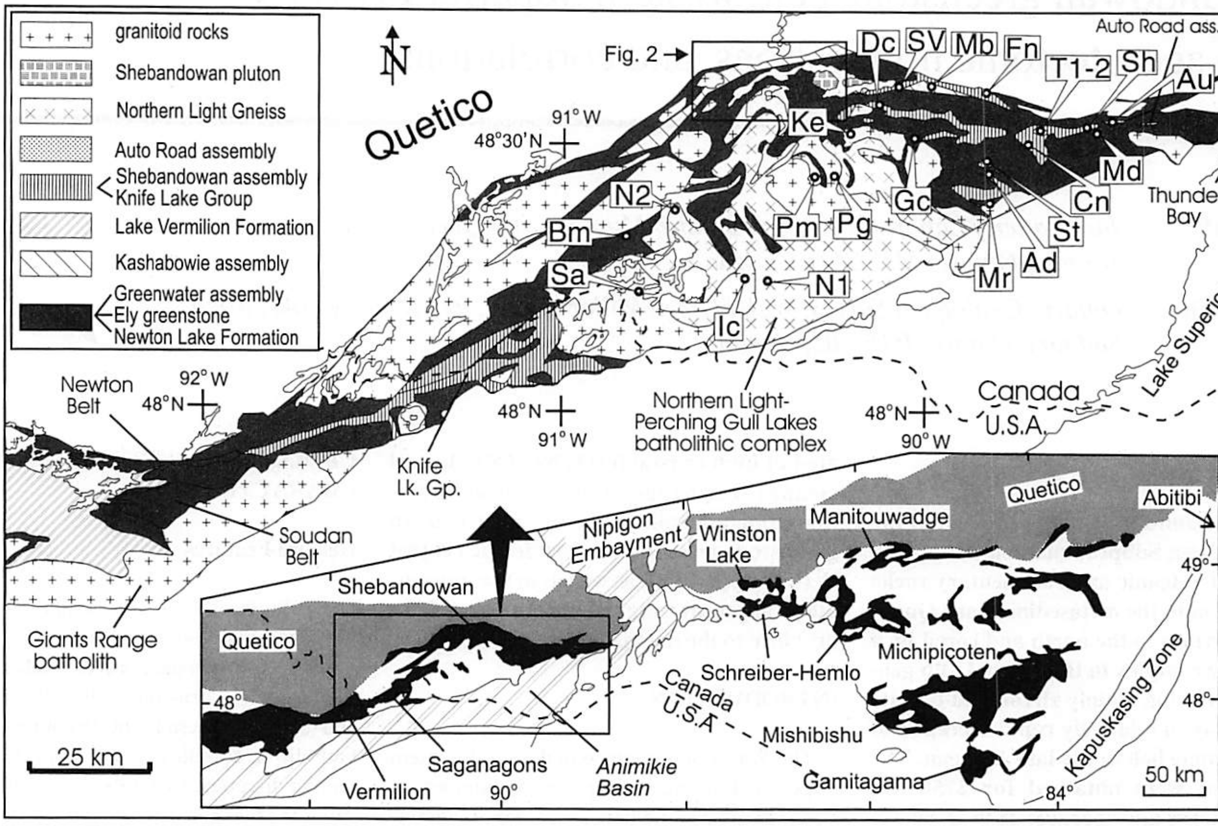


**Figure 1. Geological map of the Shebandowan and Saganagons greenstone belts, and the Vermilion district of northern Minnesota, showing main geological subdivisions and sample locations. SV—alkalic volcanic breccia, Shebandowan Group (= sample C-83-39 in Corfu and Stott, 1986); description of other samples is given in Table 1. Inset shows distribution of greenstone belts and position of map area within the Wawa Subprovince.**

blage in the Saganagons greenstone belt. More extensive recent mapping and the present geochronological survey, however, have led to a reevaluation and modifications of the proposed subdivisions. In this report, most areas previously assigned to the Burchell assemblage are now considered to be part of the Greenwater assemblage, because they are indistinguishable in terms of age—all are roughly 2720 Ma—and because, in spite of local reversals due to folding, the thicker sections of volcanic flows show consistent younging directions throughout the area. Part of the Burchell assemblage in the northern part of the belt, however, is separated into a distinct assemblage. These units consist of ca. 2695 Ma supracrustal rocks and in this paper are assigned to an (informal) "Kashabowie assemblage." This assemblage represents either an early expression of, or a distinct magmatic phase predating deposition of, the Shebandowan assemblage, which includes the "Timiskaming-type" rocks. A small sedimentary basin in the northeastern part of the area includes a distinctly younger clastic succession and is termed (informally) the "Auto Road assemblage."

## Greenwater and Saganagons Assemblages

The Greenwater assemblage comprises tholeiitic basalts with minor komatiitic basalts and associated komatiitic flows (Carter, 1985, 1986; Rogers and Berger, 1995; Osmani, 1997). Intermediate to felsic volcanic flows and pyroclastic units are intercalated with the generally more voluminous basaltic flows. The dominant east-west arrangement, apparent cyclicity, and facing directions formed the basis for the subdivision into cycles and assemblages (Williams et al., 1991). A number of felsic volcanic units have been sampled throughout the belt to verify their potential stratigraphic correlations (Figs. 1 and 2). They include a felsic tuff from a mainly intermediate to mafic volcanic succession east of Kabaigon Lake (Osmani, 1996)(samples Kb), a felsic tuff (Gc) at Gold Creek (Rogers and Berger, 1995) and a felsic tuff (Mr) from a fragmental unit south of Marks Lake (Rogers and Berger, 1995). Sample Md represents a rhyolitic flow associated with a Zn-Cu occurrence near Mud Lake (Farrow, 1993; Brown, 1995). Sample Bm represents a fragmental unit at Bemar Creek in the Saganagons Belt (Harris, 1968). Sample Sk was taken from a massive felsic flow south of Skimpole Lake. Bv1 and Bv2 represent tuffs from two sites about 10 m apart of the same pyroclastic unit near Beaver Lake, southwest of the Shebandowan Mine (Osmani and Payne, 1993).

Layered mafic plutons and thick sills of peridotitic, gabbroic, and anorthositic composition are prominent northwest of Upper Shebandowan Lake (Osmani et al., 1992) and east of Greenwater Lake (Watkinson and Irvine, 1964; Osmani and Payne, 1993; Osmani, 1997). A gabbro-peridotite sill hosts Ni-Cu-Pt-Co mineralization of the Shebandowan Mine (Osmani and Payne, 1993). The Haines gabbroic complex (Farrow, 1993) shows north-northeastern–trending layering and is composed of medium-grained, mesocratic gabbro with minor melanocratic gabbro, anorthosite, and pegmatitic domains (sample Ha; Fig. 2). Sample An was collected from a very coarse grained portion of an anorthosite sill west of Upper Shebandowan Lake (Osmani, 1997), while sample Nc represents pegmatitic gabbro at the North Coldstream Cu-Au-Ag deposits. The mineralization itself is hosted by silicified gabbro at

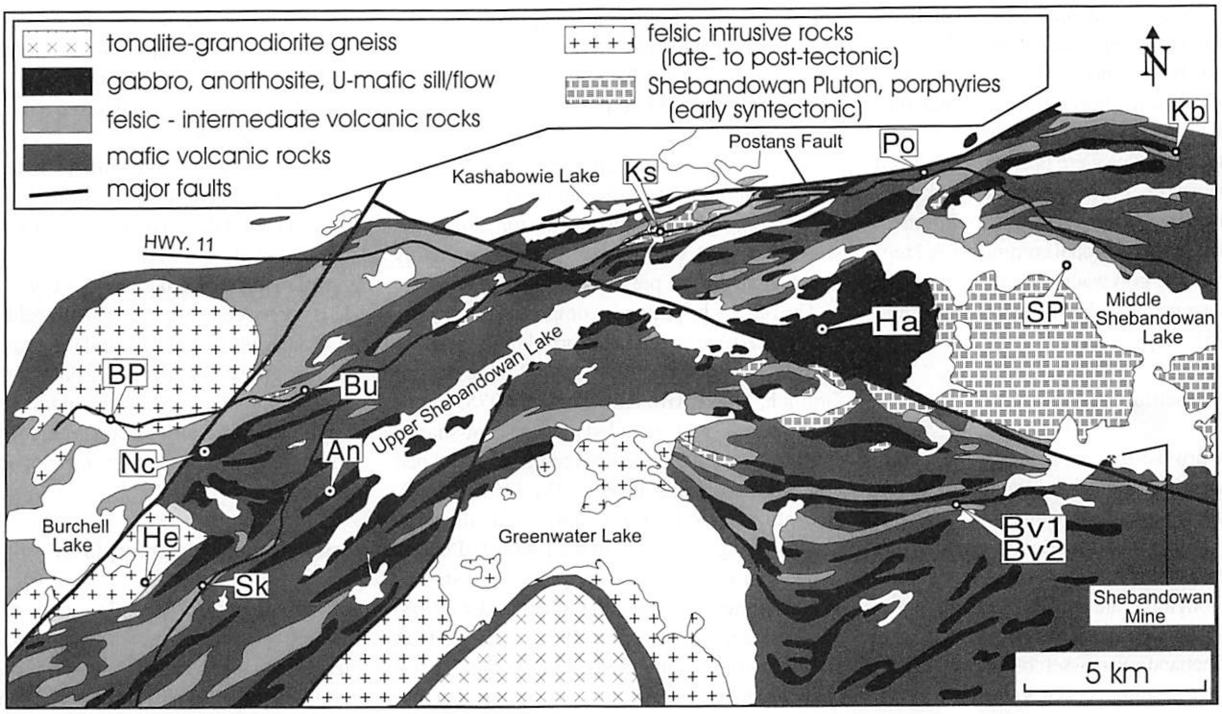


**Figure 2. Geological map of Middle–Upper Shebandowan Lakes area with main lithological subdivisions and sample locations. BP—Burchell Lake pluton, SP—Shebandowan Lake pluton (= samples C-83-36 and C-83-38, respectively, in Corfu and Stott, 1986); description of other samples is given in Table 1.**

the contact between gabbro and mafic metavolcanic rocks (Osmani et al., 1992; Farrow, 1995). All three samples are generally strongly altered with highly saussuritized plagioclase and with chlorite or amphibole as the mafic phases.

## Kashabowie Assemblage

As mentioned earlier, Kashabowie assemblage is a provisional name referring to parts of the former Burchell assemblage that are distinct in age from the Greenwater assemblage (Fig. 1). The exact distribution of the assemblage is uncertain since it appears to be tectonically interleaved with rocks of the Greenwater assemblage. One of the typical examples from this assemblage is a heterolithic volcaniclastic unit representing a debris flow, intruded by feldspar porphyry dikes east of Kashabowie (sample Ks, Fig. 2). The unit includes porphyritic rhyolite clasts with minor chert fragments and mafic clasts. Farther east along strike of this unit, finer grained, intermediate and mafic volcanic rocks are intruded by a porphyry sill (sample Po, Fig. 2), which had yielded a U-Pb age of 2733 Ma (Corfu and Stott, 1986). This age has been reassessed on the basis of new analyses in this study. Sample Bu was taken from a schistose felsic tuff representing a thick succession of felsic flows and tuffs in the northwestern part of the Shebandowan greenstone belt (Fig. 2), while sample Mb represents a very fine-grained felsic tuff located close to the inferred contact with the Shebandowan assemblage (Fig. 1).

## Shebandowan Assemblage

The Timiskaming-type assemblage is characterized by the association of calc-alkalic to alkalic mafic to felsic volcanic rocks and clastic sedimentary rocks, deposited in relatively shallow-water to subaerial environments (Shegelski, 1980). Although the contacts between the Greenwater and Shebandowan assemblages are not exposed, map patterns, structural criteria (e.g., lack of $D_1$ structures in Shebandowan assemblage domains surrounded by $D_1$-bearing deformed Greenwater assemblage rocks), and the occurrence of Greenwater assemblage clasts in Shebandowan assemblage conglomerates support the presence of an unconformity (Shegelski, 1980; Stott, 1986; Borradaile and Brown, 1987; Carter, 1985; Brown, 1995). The Shebandowan assemblage appears to form a relatively thin and often geophysically transparent apron overlying Greenwater assemblage rocks. It occurs as two main east-west–trending bands and subordinately in smaller areas in southeastern and western parts of the belt, and in general it shows remarkably little deformation (e.g., Chorlton, 1985; Carter, 1987; Brown, 1995; Rogers and Berger, 1995).

The volcanic rocks are typified by hornblende-phyric, red- to green-weathering breccias, one sample of which (SV, Fig. 1) was previously dated as 2689 +3/–2 Ma (Corfu and Stott, 1986). Several additional samples were collected in this study to evaluate possible age variations of rocks in this assemblage across the Shebandowan greenstone belt. Sample Dc represents a heterogeneous unit of graywacke intermixed with argillite and iron formation cut by red trachyte from Duckworth Township (Rogers and Berger, 1995). Three heterolithic volcanic breccias were sampled west of Stephens Lake in Adrian Township (St; Rogers and Berger, 1995), southwest of the Tower stock in Conmee Township (Cn; Carter, 1985) and on Strawberry Hill (Sh; Brown, 1995), respectively (Fig. 1). Lithologically heterogeneous samples were chosen in order to increase the chances of zircon recovery, since alkalic rocks are notoriously poor in datable zircon, although this strategy requires a grain by grain dating approach.

The Tower stock is a small body of massive, fine-grained syenite to diorite emplaced into alkalic lavas and breccias of Conmee Township. The stock and the surrounding breccias were considered by Carter (1992) to represent the high-level core of a volcanic complex. Two samples were collected for this study. T1 is a pink (biotite-) hornblende syenite collected in the western part of the body, whereas T2 represents gray biotite-clinopyroxene diorite from the monzodioritic-dioritic central region of the stock.

Finally, two samples were taken directly from sedimentary rocks. Fn represents a wacke deposited in a shallow-water, tidal-flat environment (P. W. Fralick, 1995, personal commun.). Ad represents a graphitic graywacke from a deep-water turbidite sequence at Adrian Lake (Rogers and Berger, 1995).

### Auto Road Assemblage

This is a provisional designation for a conglomeratic unit in south-central Ware Tp (Fig. 1). The map pattern suggests that this conglomerate-sandstone unit is interbedded with Greenwater assemblage basaltic units (Brown, 1995), yet the polymictic conglomerate includes feldspar-hornblende-phyric volcanic clasts typically found within the Shebandowan assemblage. Also common are coarse granitoid cobbles as well as clasts of various volcanic lithologies. The results for sandstone sample Au presented below demonstrate that this is indeed one of the youngest supracrustal units of the Shebandowan greenstone belt as well as of the neighboring Quetico Subprovince, justifying its separate designation.

### Plutonic Rocks

Plutonic rocks occur both within the Northern Light–Perching Gull Lakes batholithic complex and as discrete plutons within the Shebandowan greenstone belt. The Northern Light–Perching Gull Lakes batholithic complex consists of tonalitic gneisses intruded by mafic to felsic plutons (Percival, 1983). The Northern Light Gneiss (Grout, 1929) comprises tonalite and trondhjemite gneiss and includes sheets and xenoliths of mafic gneiss and amphibolite, which at least in part originate from the volcanic assemblages of the greenstone belt (Goldich et al., 1972; Hanson and Goldich, 1972; Arth and Hanson, 1975; Percival and Stern, 1984; Percival, 1983). The gneissosity defines dominantly northerly trends and generally wraps around the younger plutonic bodies (Percival, 1983). A previous U-Pb bulk zircon age (Hart and Davis, 1969) and Rb-Sr and K-Ar whole-rock and mineral analyses (Hanson et al., 1971) indicated formation of the gneisses ca. 2.7 Ga with mineral ages as young as 2570 Ma, and mantle-like initial Sr ratios suggesting a short crustal residence time of the protoliths. Two samples were investigated in the course of this study. N1 is a melanocratic biotite-hornblende gneiss from a relatively homogeneous outcrop cut by apophyses of the Icarus pluton (Fig. 1). N2 is a more leucocratic biotite gneiss taken from the vicinity of a subsidiary wing of the Saganaga pluton (Harris, 1968) at the northeastern end of the Saganagons belt. The relatively heterogeneous outcrop is characterized by complex folding, amphibolitic intrusions, and pervasive potassic veining, and, although only the tonalitic phase was sampled, it was not possible to completely avoid some diffuse potassic domains.

The Saganaga pluton is composed dominantly of quartz-phyric biotite-hornblende tonalite (Grout, 1929; Goldich et al., 1972; Hanson and Goldich, 1972; Arth and Hanson, 1975; Evans and Hanson, 1993) intruded as a crescent-shaped synform at the interface between greenstone belt and Northern Light Gneiss (Davidson, 1980). The pluton has been the subject of intensive geochronological studies in the 1960s. U-Pb ages were obtained as part of the pioneering studies using titanite by Tilton and Grünenfelder (1968) and Catanzaro and Hanson (1971), whereas Hart and Davis (1969) reported a U-Pb a bulk zircon analysis and Hanson et al. (1971) carried out Rb-Sr and K-Ar determinations on whole-rock and mineral systems. These studies indicated formation of the pluton ca. 2.7 Ga, an initial Sr ratio suggestive of a short-lived crustal residence time of the protolith, and a record of postmagmatic effects in mineral systems as late as 2.5 Ga. One sample (Sa) of typical tonalite was collected for this study.

The Icarus pluton is composed of a monzodiorite phase in the west and a granodiorite phase in the east (Goldich et al., 1972; Hanson and Goldich, 1972; Arth and Hanson, 1975). Early dating by U-Pb on titanite (Catanzaro and Hanson, 1971) and Rb-Sr and K-Ar on whole rocks and minerals (Hanson et al., 1971) indicated an age and Sr initial ratio indistinguishable from those of the Saganaga pluton. The sample collected for this study (Ic) is a biotite-hornblende-clinopyroxene monzodiorite with perthitic feldspar from the same site as sample NL-12 of Hanson et al. (1971).

The Kekekuab pluton is an anticlinal crescentic intrusion emplaced at the interface between Northern Light–Perching Gull Lakes batholithic complex and greenstone belt, and is composed mainly of biotite-hornblende quartz-monzonite to diorite and granodiorite (Percival et al., 1985; Rogers and Berger, 1995). One sample of hornblende granodiorite (Ke) was collected for U-Pb dating.

The Perching Gull Lake pluton is a synformal crescentic intrusion at the interior of the Northern Light–Perching Gull Lakes batholithic complex. The pluton is composed of quartz monzonite to minor diorite; it borders a mafic gneiss unit and is surrounded by a younger granite body (Stern, 1984). Sample Pm corresponds to the dominant quartz monzonite phase described by Stern (1984) with amphibole and totally chloritized biotite. A second sample (Pg) of biotite granodiorite (to granite) represents the surrounding granite pluton.

The syenitic to monzonitic Hermia stock intrudes metavolcanic successions in the northwestern part of the Shebandowan greenstone belt (Osmani et al., 1992) to the south of the mainly granitic Burchell Lake pluton (Fig. 2). Sample He is a very coarse-grained alkali-feldspar syenite with large 1–3 cm euhedral feldspar and interstitial aggregates of unaltered euhedral blue amphibole and generally altered titanite embedded in epidote and locally carbonate. Euhedral rutile, present in mineral separates, was not observed in thin section.

### Structures and Metamorphism

Mapping of the Shebandowan greenstone belt has outlined various sets of structures. $D_1$ deformation is characterized by westerly plunging mineral lineations and is recorded locally in Greenwater assemblage strata (Stott and Schwerdtner, 1981; Stott, 1986). $D_1$ did not overprint the Shebandowan pluton, and its age of 2696 ± 2 Ma (sample SP, Fig. 2) establishes therefore a minimum age for $D_1$ deformation (Corfu and Stott, 1986). The dominant structures of the Shebandowan greenstone belt are folds, steeply dipping foliations, and easterly plunging mineral lineations formed during $D_2$ (Stott and Schnieders, 1983). These structures are developed mainly in northern domains of the Shebandowan greenstone belt; in particular, they are the earliest structures recorded in the Shebandowan assemblage (Stott, 1986; Borradaile and Brown, 1987). The volcanic breccia (SV, Fig. 1) dated as 2689 +3/–2 Ma, defined an upper age limit for this event (Corfu and Stott, 1986). Within the strain aureole of late kinematic plutons such as the 2684 +6/–3 Ma Burchell Lake pluton (sample BP, Fig. 2; Corfu and Stott, 1986), the $D_1$ and $D_2$ lineations have been rotated toward subvertical attitudes. A third deformation event ($D_3$) formed steeply plunging kink folds.

The Shebandowan greenstone belt is transected by a system of northeast-striking sinistral faults and complementary northwest-striking dextral faults. The Postans fault north of Kashabowie and its extension farther east marks the boundary between the Shebandowan greenstone belt and the Quetico Subprovince (Fig. 2), but in the northwestern part of the belt the boundary zone is characterized by uniform $D_2$ structures without a major intervening fault (Stott and Schwerdtner, 1981; Borradaile and Spark, 1991).

The Shebandowan greenstone belt exhibits greenschist facies metamorphic assemblages, except within relatively narrow contact-metamorphic aureoles of plutons, where higher grade parageneses occur. Hydrothermal alteration has affected mainly shear zones in northern parts of the belt and is locally associated with Au mineralization (Chorlton, 1987). Although it is not specifically noted, all the samples of supracrustal rocks have been metamorphosed, developing sericite and chlorite in a generally weakly recrystallized matrix. The mafic minerals and plagioclase in the gabbros and anorthosite show intense retrogression to chlorite, actinolite, epidote, and carbonate. The strongest overprint is recorded in sample Be from the Saganagons belt, which shows a well-recrystallized matrix with metamorphic amphibole and titanite. More mafic sites of the outcrop are garnetiferous. This effect is probably due to contact metamorphism during intrusion of the adjacent Myrt Lake batholith. The primary mineral assemblages of the plutonic rocks are generally well preserved, but secondary sericite, chlorite, or epidote are locally present.

## ANALYTICAL PROCEDURE

The U-Pb analyses were carried out by isotope dilution following the procedure of Krogh (1973, 1982). Further details were given in Corfu and Stott (1986) and Corfu and Noble (1992). Blank corrections were ≤2 pg Pb and 0.1 pg U for zircon, and 10 pg Pb and 0.5 pg U for titanite and rutile. Initial common Pb for zircon was corrected using Pb compositions calculated using the Stacey and Kramers (1975) model for the age of the sample. Because of the high ratio of initial to radiogenic Pb, titanite and rutile ages are much more sensitive to the choice of initial common Pb than zircon. For some of the samples we measured the common Pb composition of coexisting feldspar following the method described in Corfu and Stott (1986) or we were able to base the correction on published common Pb values from the respective units. In other cases we used either an approximate average of published values from comparable units or Stacey and Kramers (1975) estimates. Details are given in Table 1 and in the following data presentation.

Decay constant are those of Jaffey et al. (1971). Discordia lines were regressed using the method of Davis (1982). Uncertainties on the isotopic ratios and the ages are given at the 2σ level.

## U-Pb RESULTS

### Greenwater Assemblage

The zircon populations from eight felsic volcanic tuffs and flows fall into two distinct morphological categories. Two of the samples (Kb and Sk) exhibit zircon crystals dominated by {100} and {101} crystal faces (Fig. 3A), which are common characteristics of zircon in felsic volcanic rocks associated with tholeiitic assemblages (e.g., Corfu and Stott, 1993; Corfu and Noble, 1992). The other six samples (Mr, Gc, Md, Bm, Bv1, and Bv2) comprise zircon populations generally showing a predominance of {010} and {211} crystal faces (Fig. 3B). This type of zircon is more common in calk-alkalic or aluminous volcanic and plutonic rocks (e.g., Corfu and Noble, 1992). The U content of the analyzed fractions is generally low, ranging from about 20 to 150 ppm, and ratios of Th/U give intermediate values of 0.2 to 1.0.

Most of the analyses for these volcanic rocks (Table 1; Fig. 4) plot on or near the Concordia curve defining coherent patterns indicative of cogenetic zircon populations. The ages determined by regression (Md, Sk) or by averaging the $^{207}Pb/^{206}Pb$ ages of concordant analyses range from 2722 to 2718 Ma with uncertainties of 1 to 3 m.y. The most complex pattern is provided by zircon from the Beaver Lake samples (Bv1 and Bv2). Analyses for sample Bv1 yielded one concordant and several variously discordant analyses that could not be unambiguously interpreted: they could indicate either the presence of one single age population affected by multiple Pb loss events, or the presence of multiple generations including an older ≥2715 Ma group and a younger ≥2689 Ma group. The first case implies extrusion of the volcanics at about the same time as the older Greenwater successions. The latter case would have suggested extrusion of the volcanic rocks in connection with the younger Kashabowie or Shebandowan assemblages. Analyses of euhedral long-prismatic crystals and of euhedral tips from the second sample from this outcrop (Bv2) provide data that, although imprecise and somewhat discordant, support a Greenwater assemblage age. The age itself can only be approximated as 2720 ± 10 Ma, by taking into account the $^{207}Pb/^{206}Pb$ ages of the concordant analyses and the general trend of the enveloping discordia lines.

The samples of pegmatitic gabbro and anorthosite (Ha, An, Nc) contain euhedral, prismatic zircon crystals (Fig. 3C), which are generally broken into angular fragments. The euhedral prisms are characterized by well-developed {100} and {101}crystal faces. Most of the analyses on the three samples were carried out using zircon fragments with U contents of 20 to more than 200 ppm, and relatively high Th/U ratios of 1 to 2. The three sets of analyses are concordant to slightly discordant and define identical ages of 2722 ± 3–2 Ma (Fig. 4).

### Kashabowie Assemblage

Because of the heterolithic composition of sample Ks, it was anticipated that the zircon population could include multiple provenances, and this expectation is borne out by the wide range of zircon types recovered (Fig. 3D). By contrast, sample Bu was from a more homogeneous though deformed site and, at first sight, this homogeneity appeared to be reflected by a relatively uniform zircon population. The zircons in sample Mb exhibit locally pronounced rounding but, in general, they have a morphologically uniform appearance. In all three zircon populations there is a preponderance of crystals with favorably developed {110} prisms and variable proportions of {101} and {211} pyramids. Measured U contents range from 20 to 170 ppm and Th/U ratios define intermediate values between 0.3 and 0.8 (Table 1).

The data for sample Ks are all concordant but define a wide range of ages between 2766 ± 2 Ma and 2695 ± 3 Ma (Fig. 5), the youngest one representing a maximum age of deposition of the volcanic unit. Sample Bu also yields a spectrum of ages, ranging from 2720 for the oldest grain to 2696 ± 3 Ma for the 0.9% discordant analysis of the youngest fraction of euhedral zircon tips. A much simpler pattern with an age of 2694 ± 2 Ma was obtained instead from four single grain analyses of sample Mb. The fourth sample in this group (Po) is the porphyry previously studied by Corfu and Stott (1986). The previous analyses had been carried out on multigrain fractions of 200–300 μg and yielded three concordant to variously discordant analyses, which were colinear and defined an upper intercept age of 2733 ± 3 Ma. The new analyses on single grains indicate, however, a large variation in ages from 2761 Ma, obtained for a single euhedral to subhedral grain, to 2710 Ma for a euhedral tip. The new data show that the previous age was a meaningless mixed age. The youngest apparent age of 2710 Ma is a maximum estimate for the emplacement of the sill, but the geochemical affinity between similar porphyries in the area and volcanic rocks of the Kashabowie assemblage (Osmani, 1996) suggest that this rock may have formed considerably later, possibly in connection with the Shebandowan pluton at around 2696 Ma.

### Shebandowan Assemblage

The zircon yield in most samples was relatively small and, as expected from the heterogeneity of the samples, most populations revealed a variety of zircon morphologies requiring a careful zircon selection.

The simplest data pattern was found in sample Dc (Table 1; Fig. 6) with four single grain analyses yielding overlapping results at 2692 ± 2 Ma, which is a maximum age for deposition of this unit. The age is consistent with the previously obtained date of 2689 +3/–2 Ma for alkalic breccia

TABLE 1. U-Pb DATA

| Mineral, properties* | Weight† (µg) | U† (ppm) | Th/U§ | Pbc# (pg) | $^{206}Pb/^{204}Pb$** | $^{206}Pb/^{238}U$†† | ±2σ§§ (abs) | $^{207}Pb/^{235}U$†† | ±2σ§§ (abs) | $^{207}Pb/^{206}Pb$†† (Ma) | ±2σ§§ (Ma) | Disc. (%) |
|---|---|---|---|---|---|---|---|---|---|---|---|---|
| Kb: felsic tuff, Kabaigon Lake (C-93-30; 704550/5394950)## | | | | | | | | | | | | |
| z eu sp [14] | 11 | 59 | 0.48 | 2.5 | 8511 | 0.5252 | 0.0024 | 13.578 | 0.070 | 2720.5 | 2.4 | 0.0 |
| z eu sp [f] | 19 | 65 | 0.49 | 1.7 | 24004 | 0.5234 | 0.0024 | 13.543 | 0.070 | 2721.9 | 2.4 | 0.4 |
| z eu sp [f] | 29 | 73 | 0.51 | 2.6 | 26846 | 0.5234 | 0.0027 | 13.545 | 0.072 | 2722.1 | 2.0 | 0.4 |
| Gc: felsic tuff, Gold Creek, Duckworth Township (C-92-9; 718540/5377720) | | | | | | | | | | | | |
| z sb [1] | 29 | 19 | 0.39 | 1.2 | 15271 | 0.5233 | 0.0024 | 13.512 | 0.071 | 2718.3 | 2.4 | 0.2 |
| z fr [1] | 6 | 30 | 0.93 | 0.7 | 7854 | 0.5214 | 0.0026 | 13.475 | 0.075 | 2719.9 | 2.6 | 0.7 |
| z eu sp [4] | 1 | 59 | 0.47 | 0.9 | 2158 | 0.5208 | 0.0031 | 13.426 | 0.089 | 2715.8 | 3.5 | 0.6 |
| z eu [1] | 16 | 50 | 0.55 | 2.1 | 12663 | 0.5200 | 0.0024 | 13.416 | 0.070 | 2717.0 | 2.4 | 0.8 |
| Mr: felsic fragmental volcanic rock, Marks Lake, Marks Township (C-92-13; 292050/5364020) | | | | | | | | | | | | |
| z eu sp [1] | 1 | 59 | 0.64 | 1.1 | 1800 | 0.5249 | 0.0029 | 13.557 | 0.085 | 2718.7 | 4.9 | −0.0 |
| z eu lp [f] | 7 | 56 | 0.81 | 4.5 | 2850 | 0.5226 | 0.0026 | 13.517 | 0.075 | 2721.3 | 2.8 | 0.5 |
| z eu sp [f] | 2 | 44 | 0.74 | 1.0 | 3620 | 0.5203 | 0.0026 | 13.468 | 0.074 | 2722.6 | 3.0 | 1.0 |
| Bm: felsic metavolcanic rock, Saganagons assemblage, Bemar Creek (C-92-26; 662820/5357150) | | | | | | | | | | | | |
| z sb [1] | 2 | 58 | 0.78 | 0.8 | 5010 | 0.5242 | 0.0027 | 13.561 | 0.075 | 2721.5 | 3.3 | 0.2 |
| z eu tip [1] | 2 | 66 | 0.48 | 0.7 | 6662 | 0.5256 | 0.0027 | 13.571 | 0.077 | 2718.1 | 2.6 | −0.2 |
| z eu tip [1] | 4 | 110 | 0.48 | 0.8 | 17294 | 0.5228 | 0.0024 | 13.502 | 0.071 | 2718.7 | 2.4 | 0.3 |
| z eu sp [1] | 1 | 53 | 0.55 | 2.0 | 889 | 0.5182 | 0.0028 | 13.421 | 0.089 | 2723.2 | 4.9 | 1.4 |
| Md: felsic flow, Mud Lake, Ware Township (C-93-25; 314630/5376980) | | | | | | | | | | | | |
| z eu tip [1] | 10 | 50 | 0.42 | 4.3 | 3835 | 0.5222 | 0.0024 | 13.455 | 0.071 | 2714.7 | 2.8 | 0.3 |
| z fr [1] | 2 | 41 | 0.75 | 1.8 | 1502 | 0.5214 | 0.0028 | 13.446 | 0.081 | 2716.3 | 3.8 | 0.5 |
| z eu tips (-lp) [f] | 3 | 125 | 0.52 | 0.8 | 15188 | 0.5193 | 0.0027 | 13.362 | 0.076 | 2712.7 | 2.6 | 0.7 |
| z eu lp [f] | 2 | 133 | 0.40 | 2.9 | 2882 | 0.5062 | 0.0024 | 12.912 | 0.071 | 2698.2 | 2.8 | 2.6 |
| Sk: felsic flow, Skimpole Lake (C-92-25; 677700/5381550) | | | | | | | | | | | | |
| z eu tips [f] | 12 | 72 | 0.51 | 1.4 | 19584 | 0.5229 | 0.0026 | 13.529 | 0.074 | 2721.7 | 2.4 | 0.5 |
| z eu sp [f] | 25 | 53 | 0.53 | 5.4 | 8064 | 0.5239 | 0.0031 | 13.552 | 0.083 | 2721.3 | 1.5 | 0.2 |
| z fr (-eu sp) [f] | 4 | 73 | 0.52 | 1.1 | 7913 | 0.5214 | 0.0024 | 13.487 | 0.071 | 2721.3 | 2.5 | 0.7 |
| z eu tips [6] | 6 | 68 | 0.49 | 2.5 | 4785 | 0.4649 | 0.0022 | 12.010 | 0.064 | 2719.2 | 2.5 | 11.4 |
| Bv1: tuff, Beaver Lake (C-92-34; 698990/53784870) | | | | | | | | | | | | |
| z sb sp [1] | 2 | 49 | 0.34 | 5.5 | 603 | 0.5241 | 0.0031 | 13.509 | 0.091 | 2715.3 | 4.4 | −0.0 |
| z eu lp-tips [1] | <1 | >16 | 0.28 | 1.1 | 496 | 0.5181 | 0.0048 | 13.310 | 0.153 | 2710.0 | 9.2 | 0.9 |
| z eu lp-tips [9] | 1 | 148 | 0.20 | 2.4 | 1953 | 0.5093 | 0.0027 | 12.915 | 0.081 | 2688.4 | 4.4 | 1.6 |
| z eu lp-fr [f] | 2 | 62 | 0.24 | 4.1 | 985 | 0.5052 | 0.0028 | 12.811 | 0.079 | 2688.6 | 3.7 | 2.4 |
| z eu lp-tips [1] | 1 | 54 | 0.24 | 1.6 | 929 | 0.4404 | 0.0030 | 11.174 | 0.091 | 2689.6 | 8.3 | 14.9 |
| Bv2: lapilli tuff, Beaver Lake (C-92-35; 698980/53784870) | | | | | | | | | | | | |
| z tips [2] | <1 | >55 | 0.45 | 7.7 | 251 | 0.5303 | 0.0040 | 13.745 | 0.123 | 2724.7 | 6.8 | −0.8 |
| z eu lp [5] | <1 | >55 | 0.41 | 0.4 | 4292 | 0.5148 | 0.0035 | 13.242 | 0.097 | 2711.9 | 3.2 | 1.6 |
| Nc: pegmatitic gabbro, North Coldstream Mine (C-93-32; 678000/5385800) | | | | | | | | | | | | |
| z fr [f] | 8 | 114 | 1.74 | 2.2 | 13710 | 0.5234 | 0.0025 | 13.539 | 0.073 | 2721.2 | 2.4 | 0.3 |
| z fr [f] | 3 | 83 | 1.71 | 1.3 | 6074 | 0.5208 | 0.0025 | 13.459 | 0.073 | 2719.6 | 2.8 | 0.8 |
| z fr [f] | 2 | 218 | 2.00 | 1.6 | 9000 | 0.5177 | 0.0024 | 13.341 | 0.071 | 2715.2 | 2.4 | 1.2 |
| Ha: gabbro pegmatite, Haines gabbroic complex (C-93-20; 695700/5390150) | | | | | | | | | | | | |
| z fr [f] | 25 | 66 | 1.30 | 1.9 | 27849 | 0.5249 | 0.0031 | 13.584 | 0.083 | 2722.1 | 1.4 | 0.1 |
| z fr-eu lp [10] | 9 | 57 | 1.02 | 11.4 | 1482 | 0.5241 | 0.0025 | 13.556 | 0.074 | 2721.1 | 2.8 | 0.2 |
| An: anorthosite, Upper Shebandowan Lake (C-93-19; 681200/5384100) | | | | | | | | | | | | |
| z fr [f] | 10 | 20 | 2.08 | 1.5 | 4498 | 0.5237 | 0.0026 | 13.550 | 0.075 | 2721.8 | 2.6 | 0.3 |
| z fr [7] | 3 | 24 | 1.96 | 3.0 | 816 | 0.5239 | 0.0033 | 13.525 | 0.106 | 2718.1 | 6.0 | 0.1 |
| z fr (eu lp) [f] | 16 | 54 | 1.24 | 9.8 | 2847 | 0.5141 | 0.0027 | 13.296 | 0.078 | 2720.9 | 3.2 | 2.1 |
| z fr [f] | 15 | 65 | 1.53 | 1.6 | 19741 | 0.5174 | 0.0024 | 13.327 | 0.069 | 2714.3 | 2.4 | 1.2 |
| Ks: fragmental volcanic, Kashabowie (C-93-31; 690600/5392150) | | | | | | | | | | | | |
| z eu tip [1] | 3 | 76 | 0.68 | 1.1 | 7023 | 0.5343 | 0.0025 | 14.203 | 0.074 | 2766.3 | 2.4 | 0.3 |
| z an [1] | 13 | 35 | 0.42 | 0.7 | 20547 | 0.5221 | 0.0024 | 13.458 | 0.069 | 2715.5 | 2.4 | 0.3 |
| z fr [1] | 2 | 15 | 0.53 | 3.6 | 299 | 0.5254 | 0.0058 | 13.516 | 0.165 | 2712.1 | 6.8 | −0.5 |
| z eu sp [1] | 1 | 24 | 0.66 | 1.0 | 795 | 0.5164 | 0.0040 | 13.146 | 0.113 | 2694.8 | 4.8 | 0.5 |
| z eu fr [1] | 3 | 35 | 0.67 | 2.2 | 1619 | 0.5170 | 0.0025 | 13.167 | 0.074 | 2695.5 | 3.4 | 0.4 |
| Bu: felsic tuff, Burchell Lake (C-92-23; 679350/5387150) | | | | | | | | | | | | |
| z eu sp [1] | 6 | 26 | 0.38 | 2.2 | 2355 | 0.5221 | 0.0025 | 13.496 | 0.075 | 2720.0 | 3.0 | 0.5 |
| z eu sp [1] | 2 | 151 | 0.40 | 1.7 | 5772 | 0.5224 | 0.0026 | 13.488 | 0.075 | 2718.1 | 3.1 | 0.4 |
| z eu fr [1] | 8 | 51 | 0.52 | 1.7 | 7639 | 0.5142 | 0.0024 | 13.262 | 0.070 | 2716.5 | 2.6 | 1.9 |
| z eu fr [1] | 11 | 22 | 0.45 | 6.2 | 1278 | 0.5222 | 0.0025 | 13.436 | 0.075 | 2712.5 | 3.0 | 0.2 |
| z eu tips [f] | 13 | 34 | 0.36 | 3.5 | 4193 | 0.5193 | 0.0028 | 13.329 | 0.078 | 2708.6 | 2.5 | 0.6 |
| z lp [20] | 1 | 173 | 0.62 | 1.2 | 4583 | 0.4991 | 0.0024 | 12.760 | 0.069 | 2702.0 | 2.6 | 4.1 |
| z eu tips [7] | 1 | 93 | 0.43 | 2.6 | 1204 | 0.5187 | 0.0027 | 13.266 | 0.080 | 2702.7 | 3.4 | 0.4 |
| z eu tips [8] | 1 | 90 | 0.49 | 1.2 | 2439 | 0.5145 | 0.0027 | 13.106 | 0.076 | 2695.9 | 3.4 | 0.9 |
| Mb: dacitic tuff, Mabella, Blackwell Township (C-92-4; 722900/5387450) | | | | | | | | | | | | |
| z eu-sb sp [1] | 4 | 17 | 0.81 | 1.0 | 2253 | 0.5182 | 0.0026 | 13.189 | 0.074 | 2694.5 | 3.0 | 0.1 |
| z eu-sb sp [1] | 4 | 35 | 0.69 | 0.8 | 6003 | 0.5182 | 0.0025 | 13.183 | 0.072 | 2693.8 | 2.6 | 0.1 |
| z eu-sb sp [1] | 4 | 24 | 0.71 | 1.4 | 2228 | 0.5133 | 0.0026 | 13.051 | 0.079 | 2692.8 | 4.3 | 1.0 |
| z eu-sb sp [1] | 5 | 25 | 0.71 | 1.3 | 3115 | 0.5134 | 0.0025 | 13.046 | 0.079 | 2691.9 | 4.3 | 0.9 |
| Po: feldspar porphyry sill, Kabaigon Bay (C-83-37; 696250/539360) | | | | | | | | | | | | |
| z eu tip [1] | 3 | 45 | 0.69 | 4.7 | 985 | 0.5352 | 0.0028 | 14.181 | 0.085 | 2760.8 | 3.1 | −0.1 |
| z eu tip [1] | 2 | 47 | 0.37 | 0.9 | 3279 | 0.5217 | 0.0027 | 13.502 | 0.093 | 2722.2 | 5.8 | 0.7 |
| z eu tip [1] | 10 | 23 | 0.39 | 0.9 | 8395 | 0.5225 | 0.0024 | 13.462 | 0.069 | 2714.6 | 2.5 | 0.2 |
| z sb-eu [1] | 19 | 26 | 0.45 | 2.2 | 7087 | 0.5207 | 0.0024 | 13.377 | 0.070 | 2710.0 | 2.4 | 0.4 |
| Dc: mixed sedimentary and alkalic volcanic rock, Duckworth Township (C-92-11; 717000/538160) | | | | | | | | | | | | |
| z eu sp [1] | 3 | 47 | 0.72 | 0.9 | 5345 | 0.5174 | 0.0024 | 13.146 | 0.069 | 2691.6 | 2.7 | 0.2 |
| z eu-sb [1] | 10 | 26 | 0.72 | 1.5 | 5582 | 0.5161 | 0.0024 | 13.113 | 0.070 | 2691.7 | 3.2 | 0.4 |
| z eu eq [1] | 9 | 29 | 1.06 | 1.0 | 8526 | 0.5146 | 0.0026 | 13.074 | 0.073 | 2691.7 | 2.5 | 0.7 |
| z eu-sb [1] | 2 | 101 | 0.79 | 2.2 | 2954 | 0.5110 | 0.0025 | 12.967 | 0.073 | 2689.7 | 3.4 | 1.3 |

TABLE 1. U-Pb DATA (*Continued*)

| Mineral, properties* | Weight† (µg) | U† (ppm) | Th/U§ | Pbc# (pg) | $^{206}Pb/^{204}Pb$** | $^{206}Pb/^{238}U$†† | ±2σ§§ (abs) | $^{207}Pb/^{235}U$†† | ±2σ§§ (abs) | $^{207}Pb/^{206}Pb$†† (Ma) | ±2σ§§ (Ma) | Disc. (%) |
|---|---|---|---|---|---|---|---|---|---|---|---|---|
| Sh: alkalic volcanic breccia, Strawberry Hill, Ware Township (C-93-26B: 312550/5377780) | | | | | | | | | | | | |
| z eu tip [1] | 1 | 60 | 0.39 | 2.8 | 732 | 0.5237 | 0.0033 | 13.555 | 0.096 | 2722.4 | 4.2 | 0.3 |
| z eu-an lp [1] | 2 | 43 | 0.59 | 1.9 | 1521 | 0.5226 | 0.0027 | 13.507 | 0.080 | 2720.0 | 3.4 | 0.4 |
| z eu fr [1] | 3 | 33 | 0.46 | 3.6 | 901 | 0.5231 | 0.0031 | 13.490 | 0.091 | 2716.4 | 3.8 | 0.2 |
| z eu fr [1] | 1 | 45 | 0.55 | 0.9 | 1691 | 0.5213 | 0.0030 | 13.430 | 0.086 | 2714.7 | 3.6 | 0.5 |
| z eu-an lp [1] | 2 | 38 | 0.46 | 1.6 | 1565 | 0.5133 | 0.0026 | 13.169 | 0.075 | 2707.7 | 3.4 | 1.7 |
| z eu tip [1] | 1 | 28 | 0.51 | 1.4 | 648 | 0.5156 | 0.0034 | 13.098 | 0.102 | 2691.5 | 5.6 | 0.5 |
| St: volcanic breccia, Stephens Lake, Adrian Township (C-92-17: 290620/5372310) | | | | | | | | | | | | |
| z eu tip [1] | <1 | >15 | 0.49 | 1.3 | 353 | 0.5233 | 0.0055 | 13.585 | 0.172 | 2727.3 | 9.8 | 0.6 |
| z eu lp fr [1] | 1 | 103 | 1.59 | 0.9 | 3801 | 0.5220 | 0.0024 | 13.517 | 0.072 | 2723.0 | 2.8 | 0.7 |
| z eu tip [1] | <1 | >100 | 0.97 | 1.6 | 2189 | 0.5214 | 0.0026 | 13.492 | 0.076 | 2722.0 | 3.0 | 0.8 |
| z eu lp fr [1] | <1 | >20 | 0.96 | 1.2 | 485 | 0.5219 | 0.0045 | 13.161 | 0.158 | 2679.1 | 12.0 | –1.3 |
| Cn: alkalic volcanic breccia; Conmee Township (C-92-2: 740700/5373550) | | | | | | | | | | | | |
| z eu sp fr [1] | <1 | >30 | 1.19 | 1.9 | 510 | 0.5234 | 0.0033 | 13.584 | 0.110 | 2726.8 | 7.1 | 0.6 |
| z eu lp fr [1] | <1 | >105 | 1.28 | 1.0 | 3257 | 0.5122 | 0.0025 | 13.157 | 0.071 | 2709.7 | 2.8 | 2.0 |
| z eu eq [1] | <1 | >120 | 1.31 | 1.9 | 1976 | 0.5110 | 0.0024 | 13.093 | 0.077 | 2705.6 | 4.1 | 2.0 |
| z eu sp fr [1] | 1 | 112 | 1.47 | 1.4 | 2504 | 0.4942 | 0.0027 | 12.559 | 0.075 | 2692.0 | 3.5 | 4.6 |
| z eu lp fr [10] | 5 | 229 | 1.58 | 7.8 | 4139 | 0.4483 | 0.0021 | 10.948 | 0.057 | 2625.9 | 2.7 | 10.8 |
| z eu lp fr [1] | 2 | 186 | 1.96 | 2.1 | 4525 | 0.4128 | 0.0019 | 9.499 | 0.049 | 2526.6 | 2.6 | 14.0 |
| T1: syenite, Tower stock, Conmee Township (C-92-3: 743750/5376700) | | | | | | | | | | | | |
| z eu sp [1] | 1 | 59 | 0.49 | 1.1 | 1831 | 0.5407 | 0.0031 | 14.497 | 0.092 | 2780.2 | 3.8 | –0.3 |
| z eu sp [1] | 4 | 22 | 1.25 | 2.5 | 1151 | 0.5018 | 0.0028 | 12.689 | 0.080 | 2683.8 | 3.6 | 2.8 |
| z eu sp [1] | <1 | >70 | 1.73 | 5.4 | 430 | 0.5008 | 0.0037 | 12.582 | 0.106 | 2673.2 | 5.0 | 2.6 |
| z eu fr [1] | 1 | 57 | 1.63 | 1.2 | 1483 | 0.4960 | 0.0027 | 12.444 | 0.079 | 2670.8 | 4.2 | 3.4 |
| z eu eq [18] | 2 | 201 | 1.59 | 7.5 | 1512 | 0.4438 | 0.0021 | 10.504 | 0.058 | 2573.7 | 3.0 | 9.5 |
| t fr br-lbr [f] †† | 12 | 48 | 4.19 | 20.7 | 919 | 0.5129 | 0.0029 | 13.032 | 0.087 | 2691.7 | 3.8 | 1.0 |
| T2: diorite, Tower stock, Conmee Township (C-93-27: 743050/5377100) | | | | | | | | | | | | |
| z fr (ovg?)[1] | 2 | 282 | 1.19 | 1.9 | 9498 | 0.5156 | 0.0025 | 13.086 | 0.072 | 2689.8 | 2.4 | 0.4 |
| z eu sp [1] | 4 | 297 | 1.15 | 2.5 | 14969 | 0.5067 | 0.0025 | 12.793 | 0.070 | 2681.4 | 2.4 | 1.8 |
| z fr (ovg?)[1] | 2 | 323 | 1.30 | 3.4 | 5995 | 0.5066 | 0.0023 | 12.761 | 0.067 | 2677.5 | 2.4 | 1.6 |
| z fr (ovg?)[1] | 1 | 307 | 1.93 | 1.8 | 5221 | 0.4869 | 0.0022 | 12.111 | 0.063 | 2656.7 | 2.6 | 4.5 |
| z eu fr [1] | 5 | 297 | 1.85 | 3.9 | 10565 | 0.4389 | 0.0021 | 10.564 | 0.057 | 2601.9 | 2.4 | 11.7 |
| Ad: greywacke, Adrian Lake, Adrian Township (C-92-15: 291380/5369940) | | | | | | | | | | | | |
| z an [1] | 4 | 21 | 0.67 | 1.1 | 2529 | 0.5512 | 0.0028 | 15.245 | 0.088 | 2830.9 | 3.1 | 0.0 |
| z an [1] | 5 | 28 | 0.82 | 0.7 | 6431 | 0.5479 | 0.0028 | 15.139 | 0.086 | 2829.3 | 2.5 | 0.6 |
| z eu sp [1] | 3 | 34 | 0.59 | 1.3 | 2556 | 0.5244 | 0.0026 | 13.570 | 0.077 | 2722.1 | 3.0 | 0.2 |
| z eu sp [1] | 2 | 52 | 0.42 | 3.2 | 1066 | 0.5235 | 0.0030 | 13.496 | 0.086 | 2715.9 | 3.2 | 0.0 |
| z eu sp [1] | 9 | 20 | 0.46 | 0.7 | 7836 | 0.5207 | 0.0025 | 13.359 | 0.073 | 2707.9 | 2.4 | 0.3 |
| z an [1] | 5 | 30 | 0.49 | 6.8 | 733 | 0.5191 | 0.0030 | 13.259 | 0.086 | 2700.4 | 3.7 | 0.2 |
| z an [1] | 2 | 13 | 0.80 | 1.5 | 603 | 0.5190 | 0.0033 | 13.245 | 0.119 | 2699.1 | 7.9 | 0.2 |
| Fn: sandstone, Finmark Road, Highway 11-17 (C-95-20: W 89º47.945/N48º34.500) | | | | | | | | | | | | |
| z eu-sb sp [1] | 1 | 44 | 1.02 | 1.1 | 1358 | 0.5152 | 0.0033 | 13.133 | 0.093 | 2697.2 | 4.2 | 0.8 |
| z eu-sb sp [1] | 2 | 44 | 0.93 | 1.0 | 2898 | 0.5170 | 0.0025 | 13.134 | 0.071 | 2691.3 | 2.8 | 0.2 |
| z eu eq [1] | 4 | 18 | 0.95 | 0.6 | 3911 | 0.5172 | 0.0025 | 13.135 | 0.073 | 2691.2 | 2.7 | 0.2 |
| z eu eq [1] | 3 | 33 | 0.91 | 0.9 | 3516 | 0.5182 | 0.0027 | 13.159 | 0.076 | 2690.7 | 2.7 | –0.0 |
| z eu-sb sp [1] | 7 | 45 | 1.00 | 4.6 | 2173 | 0.5083 | 0.0026 | 12.891 | 0.073 | 2688.8 | 2.9 | 1.8 |
| t fr an br [1] | 2 | 48 | 1.71 | 3.4 | 953 | 0.5187 | 0.0030 | 13.175 | 0.088 | 2691.2 | 4.3 | –0.1 |
| t fr an br-rd [1] | 7 | 133 | 1.05 | 11.3 | 2691 | 0.5201 | 0.0024 | 13.199 | 0.070 | 2689.9 | 2.6 | –0.4 |
| Au: sandstone, Auto Road, Ware Township (C-93-22: 316050/5378180) | | | | | | | | | | | | |
| z sb-an [1] | <1 | >20 | 0.57 | 1.3 | 456 | 0.5218 | 0.0047 | 13.566 | 0.146 | 2729.5 | 8.0 | 1.0 |
| z sb-an [1] | <1 | >10 | 0.71 | 2.9 | 137 | 0.5279 | 0.0144 | 13.704 | 0.426 | 2727.2 | 21.5 | –0.2 |
| z sb-an [1] | 2 | 96 | 0.87 | 8.5 | 747 | 0.5171 | 0.0026 | 13.138 | 0.079 | 2691.8 | 3.7 | 0.2 |
| z eu sp [1] | 2 | 90 | 0.93 | 1.6 | 3589 | 0.5164 | 0.0024 | 13.089 | 0.069 | 2687.6 | 2.7 | 0.2 |
| z eu sp [1] | 3 | 96 | 1.00 | 10.8 | 881 | 0.5167 | 0.0025 | 13.093 | 0.073 | 2687.3 | 3.5 | 0.0 |
| z eu sp [1] | 1 | 86 | 0.89 | 2.0 | 1370 | 0.5081 | 0.0026 | 12.861 | 0.076 | 2685.3 | 3.7 | 1.7 |
| z eu sp [1] | 1 | 128 | 0.88 | 3.8 | 1116 | 0.5150 | 0.0027 | 13.024 | 0.078 | 2684.0 | 3.5 | 0.3 |
| z eu sp [1] | 1 | 157 | 1.15 | 1.1 | 4757 | 0.5147 | 0.0025 | 13.001 | 0.070 | 2681.9 | 2.9 | 0.2 |
| z eu sp [1] | 1 | 173 | 0.99 | 2.2 | 2542 | 0.5112 | 0.0024 | 12.910 | 0.069 | 2681.7 | 2.8 | 0.9 |
| N1: Northern Light tonalite gneiss, Jones Lake (C-92-32: 690200/5342030) | | | | | | | | | | | | |
| z sb [1] | 4 | 42 | 0.69 | 0.9 | 5944 | 0.5303 | 0.0025 | 13.970 | 0.074 | 2751.1 | 2.5 | 0.4 |
| z sb [1] | 1 | 116 | 0.92 | 0.9 | 4236 | 0.5305 | 0.0027 | 13.957 | 0.080 | 2749.2 | 2.8 | 0.3 |
| t fr-an br [f] | 116 | 134 | 0.24 | 74.8 | 6755 | 0.5174 | 0.0022 | 13.070 | 0.059 | 2682.2 | 1.4 | –0.3 |
| N2: Northern Light tonalite gneiss, Plummes Lake (C-92-28: 669550/5361180) | | | | | | | | | | | | |
| z eu sp [1] | 4 | 21 | 0.00 | 1.4 | 1993 | 0.5177 | 0.0026 | 13.270 | 0.077 | 2706.2 | 3.3 | 0.7 |
| z eu tip [1] | 2 | 42 | 0.01 | 1.4 | 2015 | 0.5155 | 0.0026 | 13.219 | 0.077 | 2707.1 | 3.1 | 1.2 |
| z eu tip [1] | <1 | >24 | 0.04 | 0.8 | 1004 | 0.5142 | 0.0043 | 13.323 | 0.153 | 2724.0 | 10.7 | 2.2 |
| z eu lp [1] | 1 | 16 | 0.00 | 1.6 | 347 | 0.5127 | 0.0049 | 13.622 | 0.196 | 2765.2 | 14.5 | 4.3 |
| z eu lp [1] | 1 | 17 | 0.03 | 1.9 | 295 | 0.5045 | 0.0045 | 13.883 | 0.174 | 2822.9 | 11.7 | 8.2 |
| t fr lbr [f] | 329 | 47 | 0.50 | 390.7 | 1291 | 0.5165 | 0.0017 | 13.110 | 0.050 | 2690.2 | 2.1 | 0.3 |
| t fr lbr [f] | 312 | 43 | 0.52 | 332.2 | 1327 | 0.5172 | 0.0028 | 13.128 | 0.074 | 2690.1 | 2.0 | 0.1 |
| Sa: qtz-phyric tonalite, Saganaga pluton (C-92-30: 664250/5343880) | | | | | | | | | | | | |
| z eu sp [1] | 17 | 55 | 0.66 | 1.3 | 23941 | 0.5155 | 0.0017 | 13.078 | 0.047 | 2689.1 | 1.6 | 0.4 |
| z eu sp [f] | 6 | 54 | 0.77 | 1.0 | 10725 | 0.5137 | 0.0027 | 13.033 | 0.075 | 2689.5 | 2.8 | 0.8 |
| z eu sp [f] | 3 | 56 | 0.75 | 0.6 | 9839 | 0.5113 | 0.0025 | 12.956 | 0.071 | 2687.2 | 2.8 | 1.1 |
| t sb lbr [f]†† | 237 | 23 | 2.18 | 265.5 | 686 | 0.5171 | 0.0028 | 13.106 | 0.075 | 2687.7 | 2.6 | 0.0 |
| t sb lbr [f]†† | 241 | 17 | 1.98 | 143.4 | 956 | 0.5167 | 0.0028 | 13.106 | 0.073 | 2688.8 | 2.4 | 0.2 |

TABLE 1. U-Pb DATA (*Continued*)

| Mineral, properties* | Weight† (μg) | U† (ppm) | Th/U§ | Pbc# (pg) | $^{206}Pb/^{204}Pb$** | $^{206}Pb/^{238}U$†† | ±2σ§§ (abs) | $^{207}Pb/^{235}U$†† | ±2σ§§ (abs) | $^{207}Pb/^{206}Pb$†† (Ma) | ±2σ§§ (Ma) | Disc. (%) |
|---|---|---|---|---|---|---|---|---|---|---|---|---|
| Ic: monzodiorite, Icarus pluton, Sunbow Lake (C-92-31; 684760/5347250) | | | | | | | | | | | | |
| z fr [1] | 28 | 92 | 1.15 | 1.7 | 49422 | 0.5155 | 0.0023 | 13.034 | 0.061 | 2683.8 | 1.3 | 0.2 |
| z fr [1] | 38 | 54 | 1.22 | 1.3 | 50419 | 0.5146 | 0.0025 | 13.007 | 0.071 | 2683.2 | 2.3 | 0.3 |
| t lbr [f]†† | 110 | 33 | 1.44 | 305.0 | 403 | 0.5161 | 0.0540 | 13.066 | 0.145 | 2685.8 | 4.8 | 0.1 |
| t lbr [f]†† | 134 | 24 | 0.92 | 348.6 | 313 | 0.5118 | 0.0031 | 12.951 | 0.087 | 2685.0 | 4.6 | 0.9 |
| He: syenite, Hermia stock (C-92-24; 677150/5382300) | | | | | | | | | | | | |
| z eu sp-co [6] | 1 | 191 | 1.19 | 1.3 | 4887 | 0.5129 | 0.0025 | 12.942 | 0.071 | 2680.4 | 2.6 | 0.5 |
| z eu fr [7] | <1 | >85 | 1.01 | 0.6 | 4322 | 0.5111 | 0.0027 | 12.924 | 0.078 | 2684.0 | 3.5 | 1.0 |
| z co-ovg [1] | 3 | 119 | 0.71 | 1.2 | 9402 | 0.5091 | 0.0026 | 12.846 | 0.073 | 2680.4 | 2.6 | 1.3 |
| z eu fr [f] | 9 | 156 | 1.01 | 2.1 | 20862 | 0.5069 | 0.0026 | 12.752 | 0.072 | 2675.3 | 2.6 | 1.5 |
| z eu fr [3] | 5 | 148 | 0.90 | 2.1 | 11180 | 0.5050 | 0.0024 | 12.718 | 0.067 | 2677.1 | 2.5 | 1.9 |
| r eu lp y-or [20]†† | 22 | 7 | 2.11 | 40.0 | 135 | 0.5196 | 0.0061 | 13.187 | 0.184 | 2689.7 | 9.2 | –0.4 |
| r eu lp y-or [f]†† | 45 | 5 | 1.11 | 34.4 | 240 | 0.5195 | 0.0024 | 13.165 | 0.135 | 2687.6 | 6.6 | –0.4 |
| r eu lp y-or [f]†† | 142 | 6 | 1.71 | 64.5 | 423 | 0.5051 | 0.0027 | 12.741 | 0.080 | 2679.7 | 2.2 | 2.0 |
| t br [20]†† | 32 | 20 | 7.43 | 86.2 | 249 | 0.5073 | 0.0029 | 12.786 | 0.092 | 2678.4 | 5.0 | 1.5 |
| t br [f]†† | 22 | 18 | 7.17 | 75.6 | 175 | 0.4822 | 0.0032 | 12.151 | 0.112 | 2678.0 | 6.8 | 6.4 |
| Ke: granodiorite, Kekekuab pluton, Matawin River (C-92-12; 718530/5373000) | | | | | | | | | | | | |
| z eu sp [1] | 7 | 113 | 0.88 | 1.3 | 20055 | 0.5119 | 0.0025 | 12.972 | 0.070 | 2687.3 | 2.5 | 1.0 |
| z eu sp [1] | 11 | 81 | 0.70 | 22.8 | 1278 | 0.5143 | 0.0027 | 13.001 | 0.074 | 2683.4 | 2.9 | 0.4 |
| z eu sp [f] | 8 | 79 | 0.83 | 7.9 | 2625 | 0.5129 | 0.0029 | 12.973 | 0.081 | 2684.2 | 2.6 | 0.7 |
| z eu sp [f] | 16 | 57 | 0.83 | 2.2 | 13437 | 0.5113 | 0.0025 | 12.918 | 0.070 | 2682.6 | 2.7 | 0.9 |
| t fr br-rd [f]†† | 237 | 67 | 4.51 | 339.5 | 1535 | 0.5163 | 0.0016 | 13.056 | 0.045 | 2684.0 | 1.8 | 0.0 |
| t fr br-rd [f]†† | 137 | 69 | 4.59 | 233.8 | 1311 | 0.5111 | 0.0052 | 12.919 | 0.138 | 2683.1 | 3.8 | 1.0 |
| Pm: quartz-monzonite, Perching Gull Lake pluton, Swallow Lake (C-92-20; 698620/5368580) | | | | | | | | | | | | |
| z eu sp [1] | 7 | 42 | 0.56 | 1.8 | 5334 | 0.5147 | 0.0024 | 12.991 | 0.069 | 2680.6 | 2.6 | 0.2 |
| z eu sp [fr] | 4 | 137 | 0.82 | 0.8 | 17750 | 0.4959 | 0.0025 | 12.479 | 0.069 | 2675.7 | 2.6 | 3.6 |
| t fr br [f]†† | 227 | 40 | 6.49 | 425.0 | 705 | 0.5129 | 0.0018 | 12.933 | 0.052 | 2679.1 | 2.8 | 0.5 |
| t fr br [f]†† | 317 | 33 | 7.00 | 522.0 | 657 | 0.5125 | 0.0480 | 12.920 | 0.128 | 2678.8 | 4.4 | 0.5 |
| Pg: granodiorite, Perching Gull Lake pluton, Kegmus Lake (C-92-19; 702800/5369550) | | | | | | | | | | | | |
| z eu fr (ovg?)[1] | 5 | 20 | 0.30 | 1.3 | 2553 | 0.5166 | 0.0025 | 13.188 | 0.073 | 2699.4 | 3.0 | 0.7 |
| z eu fr (ovg?)[1] | 1 | 43 | 0.89 | 1.3 | 1056 | 0.5187 | 0.0030 | 13.184 | 0.088 | 2692.2 | 4.3 | –0.0 |
| z eu tip [1] | 3 | 49 | 0.82 | 1.2 | 3926 | 0.5144 | 0.0024 | 13.072 | 0.070 | 2692.1 | 2.8 | 0.8 |
| z eu tip [1] | 11 | 106 | 1.10 | 2.0 | 19190 | 0.5162 | 0.0028 | 13.017 | 0.071 | 2679.4 | 2.6 | –0.2 |
| z eu lp [f] | 1 | 88 | 0.74 | 3.1 | 925 | 0.5028 | 0.0030 | 12.664 | 0.085 | 2677.3 | 3.5 | 2.3 |
| t fr-eu lbr [f]†† | 191 | 30 | 2.09 | 578.2 | 328 | 0.5136 | 0.0025 | 13.003 | 0.071 | 2685.7 | 3.2 | 0.6 |
| t fr-eu lbr [f]†† | 24 | 25 | 1.10 | 58.4 | 342 | 0.5152 | 0.0028 | 13.015 | 0.088 | 2682.1 | 4.4 | 0.2 |

*z = zircon, t = titanite, r = rutile; all minerals abraded prior to analysis (Krogh 1982); eu = euhedral, sb = subhedral, an = anhedral eq = equant, lp = long-prismatic, sp = short-prismatic; fr = fragments or broken prisms; br = brown, rd = red, lbr = light brown, y = yellow, or = orange, co = core, ovgr = overgrowth, tip = tip, [n] = number of grains (f = >30 grains).

†Weights are known to be better than 10% when over 10 μg, and about 50% when less than 2 μg; accuracy of U-concentration is roughly proportional to uncertainty of sample weight.

§Model Th/U ratio estimated from $^{208}Pb/^{206}Pb$ ratio and age of sample.

#Total common Pb in sample, includes initial and blank Pb.

**Corrected for spike and fractionation.

††Corrected for spike, fractionation, blank and initial common Pb, which is estimated using model of Stacey and Kramers (1975), except for titanite in samples T1, Ke and Pm corrected using: 6/4 = 13.5 (±1%), 7/4 = 14.5 (±1%), 8/4 = 33.43 (±1%); titanites in samples Sa and Ic corrected using: 6/4 = 13.37 (±0.6%), 7/4 = 14.43 (±0.6%); 8/4 = 33.09 (±1%) (Icarus pluton, Arth and Hanson (1975)); titanite in sample Pg corrected using: 6/4 = 13.487 (±0.09%), 7/4 = 14.587 (±0.16%), 8/4 = 33.294 (±0.25%) (K-feldspar residue, sample Pg, this study); and titanite in sample He corrected using: 6/4 = 13.559 (±0.3%), 7/4 = 14.648 (±0.3%), 8/4 = 33.370 (±0.4%) (Burchell Lake pluton, Corfu and Stott (1986)); Pb composition of K-feldspar in sample He is: 6/4 = 14.016 (±0.09%), 7/4 = 14.709 (±0.16%), 8/4 = 33.601 (±0.25%) for residue after leaching and 6/4 = 14.349 (±0.11%), 7/4 = 14.756 (±0.18%), 8/4 = 33.827 (±0.27%) for leachate (this study).

§§2σ uncertainty calculated by error propagation procedure that takes into account internal measurement statistics and external reproducibility, as well as uncertainties in the blank and common Pb correction.

##Coordinates: Easting and Northing, UTM Zones 15/16, NTS Reference 52.

(SV) at Lower Shebandowan Lake (Corfu and Stott, 1986), suggesting a provenance of the grains from coeval Shebandowan assemblage eruptions.

Five of six analyses of single zircon grains from sample Sh are concordant but define a range of ages. Four analyses are grouped between 2722 and 2715 Ma and presumably reflect the incorporation of xenocrystic or detrital grains derived from the older Greenwater assemblage. The youngest grain yields an age of 2692 ± 6 Ma, which overlaps the period of Shebandowan volcanism determined elsewhere in the Shebandowan greenstone belt.

The attempt to extract information from breccia St was not very successful. The sample contained only a small amount of zircon grains, four of which were analyzed. Three of the analyses cluster at about 2723 Ma, whereas the fourth is reversely discordant with a $^{207}Pb/^{206}Pb$ age of 2679 ± 12 Ma. This imprecise date tends to confirm a Shebandowan assemblage affinity of the breccia, whereas the older grains indicate provenance from the underlying Greenwater assemblage.

Six analyses were carried out on zircon of sample Cn. One of the data points is concordant at about 2727 Ma. All the other analyses are 2% to 14% discordant. Five of the data points define a colinear array (40% fit) with an upper intercept at 2726 ± 5 Ma and a lower intercept age of 1130 Ma. The most discordant analysis deviates to the left of the line, indicating more complex Pb loss or a younger initial age. The zircons show con-

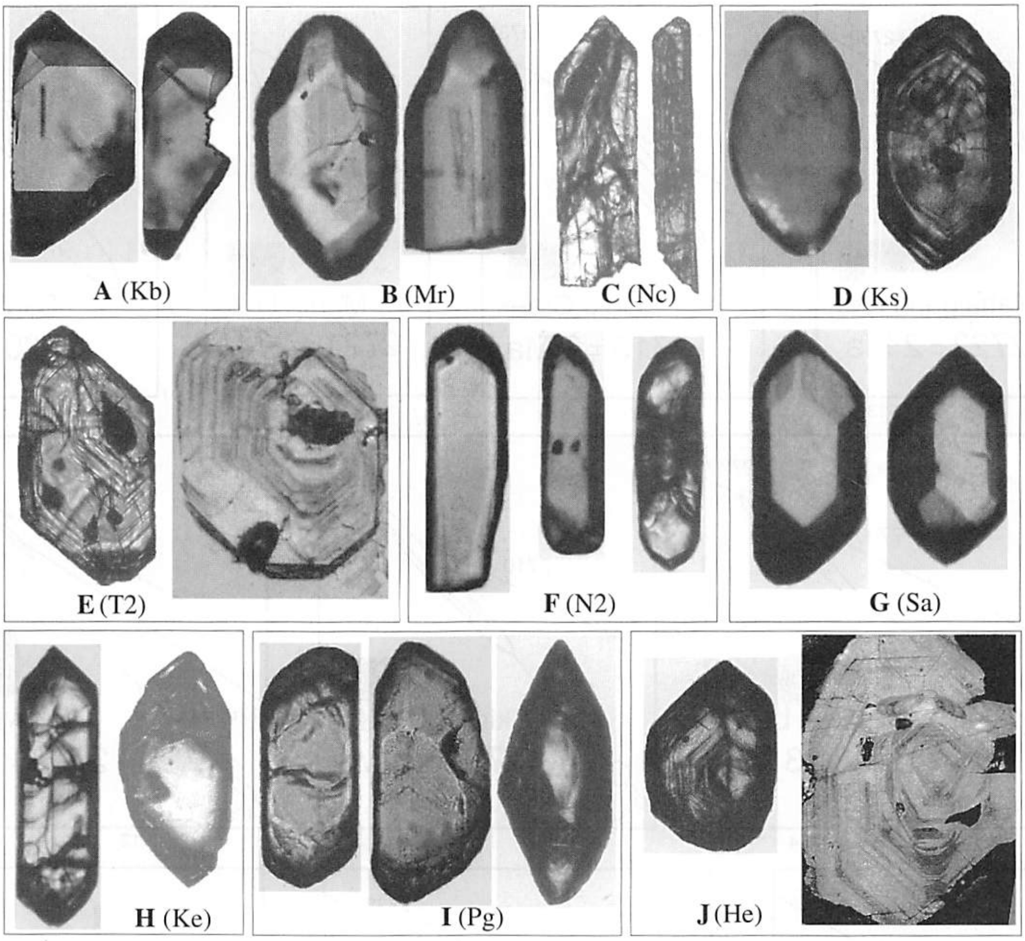


**Figure 3. Typical zircon morphologies and textures (see text for details). (A–B) Main zircon types in volcanic rocks. (C) Euhedral, prismatic crystals in gabbros and anorthosite displaying widespread fracturing and fragmentation. (D) Subrounded grain (left) and euhedral, zoned crystal (right) from mixed population of volcaniclastic sample Ks. (E) Euhedral crystals of Tower stock showing oscillatory zoning and dark inclusions. (F) Euhedral prisms, one of them with visible core, in Northern Light Gneiss. (G) Euhedral crystals of Saganaga tonalite. (H–I) Typical zircon in Kekekuab and Perching Gull Lake plutons; euhedral, core-free crystals to the left and grains with large cores to the right. (J) Euhedral zircon with complex zoning in Hermia syenite. The grains are about 100–150 μm in size and viewed in transmitted light except right-hand side grains in E and J, which were taken in reflected light from HF-etched, polished grain mounts.**

sistently high Th/U ratios supporting a provenance from a unique source. These relationships can be interpreted in one of two ways: (1) the zircons are indigenous components of the volcanic breccia, thus this phase of alkalic volcanism occurred broadly in connection with Greenwater assemblage magmatism, as suggested by Carter (1987); or (2) the zircons are xenocrystic components of the breccia and were derived from the volcanic substratum.

To further evaluate these alternatives we determined the age of the Tower stock, which intrudes the center of the Conmee volcanic succession, and appears to represent the central plug of the volcanic complex. Syenite T1 contained a population of generally U-rich, zoned, and fractured zircons, locally containing visible cores, which are inherited xenocrysts as shown by one analysis at 2780 Ma. The other zircon analyses are between 2.6% and 9.5% discordant and somewhat scattered. Small amounts of titanite were also present in this rock, yielding a 1% discordant data point with a $^{207}Pb/^{206}Pb$ age of 2691 ± 4 Ma. The zircon population in diorite sample T2 provided more suitable choices for targeting the analyses on core-free portions of crystals (Fig. 3E). Only one of the analyses is concordant while the others are between 2% and 12% discordant, but the five data points define a collinear array (22% fit) with an upper intercept age of 2690 ± 3 Ma and a lower intercept age of about 1000 Ma. Two of the least discordant analyses of sample T1 also overlap this line and together with the titanite age support the coeval origin of the two phases. The age of 2690 Ma confirms a syn-Shebandowan assemblage affinity of the stock, and indirectly argues for a similar age for the Conmee volcanic breccia Cn, implying that the 2726 Ma age dates a xenocrystic component.

Of the seven analyses carried out on single detrital zircons from graywacke Ad, two yield overlapping ages of about 2830 Ma, whereas the others range in age between 2722 and 2699 Ma. The two youngest at 2700 ± 4 and 2699 ± 8 Ma, define a maximum age of sedimentation. The Adrian Lake turbidite succession is therefore definitively younger than the Greenwater assemblage, but the data permit a deposition of the sediments prior to that of the Shebandowan assemblage.

Five zircon and two titanite grains were analyzed in sample Fn. The titanite and three of the zircon grains plot concordantly at 2691–2690 Ma. Another zircon analysis is 1.8% discordant

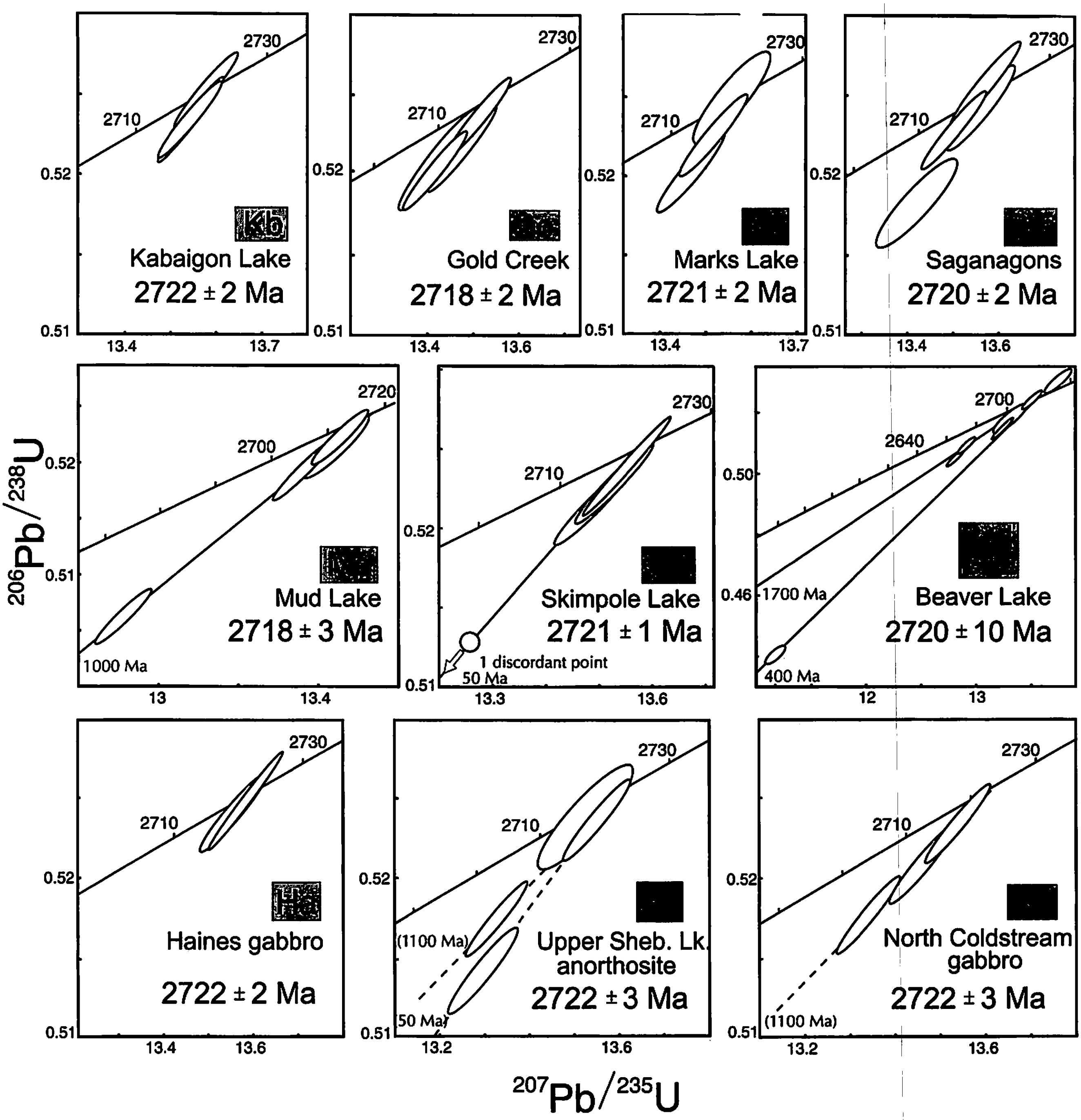


**Figure 4. Concordia diagrams with U-Pb analyses for zircon from volcanic rock samples of the Greenwater assemblage and from related gabbroic and anorthositic intrusions. Ellipses in this and the following diagrams indicate 2σ.**

and has a $^{207}Pb/^{206}Pb$ age of 2689 Ma. Only the fifth zircon grain exhibits a somewhat older age of 2697 Ma. Because we addressed mainly the age of deposition, the selected zircons were biased in favor of those showing shapes and types of inclusions frequently seen in zircon of alkalic igneous rocks. Thus, the abundance of "young" zircons does not necessarily reflect the real age distribution of the population. The ease with which these "young" zircons could be found suggests nevertheless that much of the detritus was derived from erosion of Shebandowan assemblage rocks and that the shallow-water succession may have been deposited during active volcanism. These relationships are comparable to those observed for the Timiskaming assemblage in the Abitibi greenstone belt (Corfu et al., 1991).

**Auto Road Assemblage**

Nine analyses were carried out on detrital zircons from sample Au (Fig. 6). Two of the grains define imprecise ages of 2730 to 2727 Ma whereas the others range from 2692 to 2682 Ma. The two youngest grains at 2682 ± 3 Ma clearly postdate the time of deposition of the Shebandowan assemblage.

### Northern Light–Perching Gull Lakes Batholith and Late Tectonic Plutons

Sample N1 of the Northern Light Gneiss yields a zircon population of mainly subhedral grains. Two zircon analyses yield concordant data indicating an age of 2750 ± 2 Ma (Fig. 7). Coexisting titanite is much younger at 2682 ± 2 Ma and reflects metamorphic crystallization in connection with the younger plutonic events of the area.

The second tonalitic sample N2 contains largely euhedral prismatic zircon crystals with well-developed {110} prisms and variable combinations of {101} and {211} pyramids indicative of a homogeneous magmatic population, but local anhedral cores and subrounded grains also occur (Fig. 3F). The zircon analyses yield a complex pattern whose significance is not clearly understood. One euhedral crystal and a similar crystal tip define overlapping, slightly discordant data with a $^{207}Pb/^{206}Pb$ age of about 2707 Ma. Three further analyses yield data points that are more discordant and have older $^{207}Pb/^{206}Pb$ ages. All the grains exhibit extremely low Th/U, which is a common characteristic of highly evolved granitic melts. The data pattern suggests the presence of inherited components older than 2823 Ma in a ≤2707 Ma zircon population, which would be consistent with the observation of cores in the population. Nevertheless, some aspects of the data remain puzzling, in particular the fact that the analyses are discordant in spite of having low U contents, and in spite of the homogeneity and lack of cracks and of alteration of the selected grains. As an alternative to inheritance, the pattern may indicate the presence of unsupported $^{207}Pb$ in zircon, as documented by Mortensen et al. (1992). A minimum age for formation of the rock and its gneissification is provided by coexisting titanite with a concordant age of 2690 ± 2 Ma.

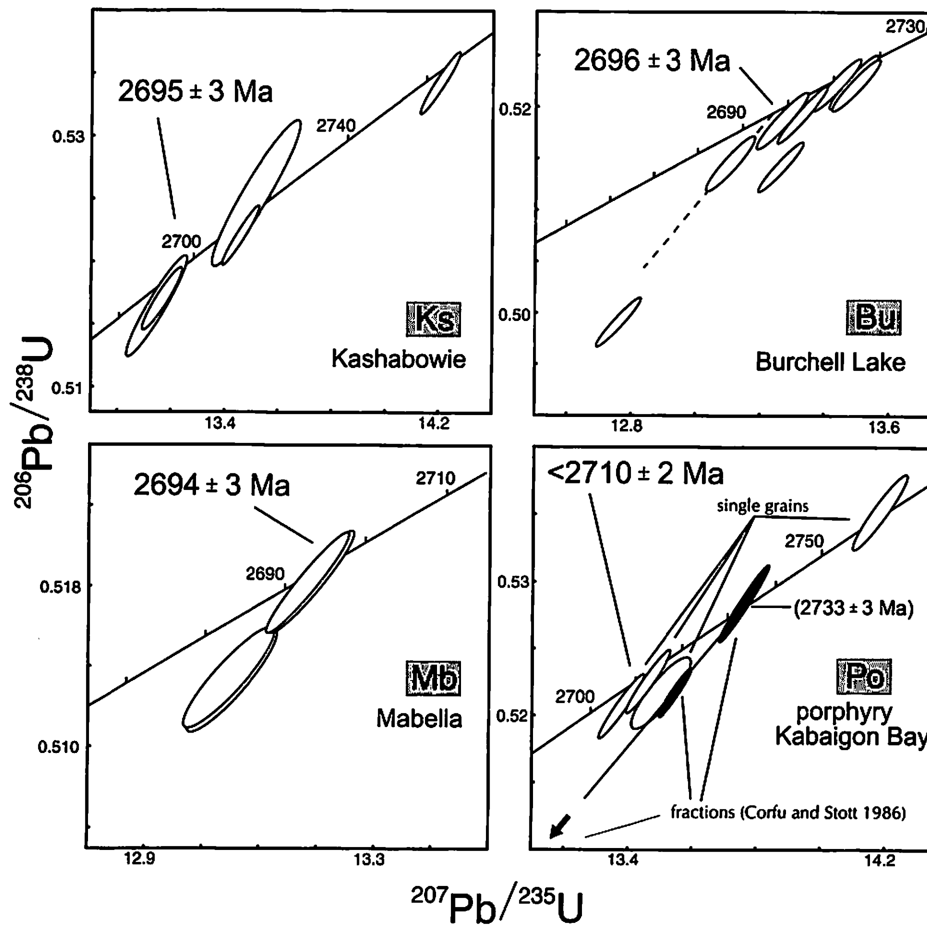


**Figure 5. Concordia diagrams with U-Pb analyses for zircon from volcanic rock samples and a feldspar porphyry of Kashabowie assemblage.**

Samples of the Saganaga (Sa), Icarus (Ic), Kekekuab (Ke), and Perching Gull Lake plutons (Pm and Pg) all contain somewhat comparable zircon populations. These are composed mainly of euhedral, relatively short-prismatic crystals showing a mixed development of the {100} and {110} prismatic and {101} and {211} pyramidal faces, with {110} and {211} being most prominent in sample Sa and least prominent in Ic and Pm (Fig. 3, G–I). Cores can be seen in samples Ic, Ke, and Pg (Fig. 3, H–I). The scatter of the data in sample Pg and the slight deviation of one analysis in sample Ke demonstrate that these cores are inherited xenocrysts. Otherwise, the zircon data in all five samples establish well-constrained ages ranging from 2689 ± 1 for Sa to 2680 ± 2 Ma for Pg (Fig. 7). The titanite data for these samples are much more strongly dependent on uncertainties introduced by the corrections for initial Pb than zircon. Initial Pb is known for the Icarus pluton (Arth and Hanson, 1975; IC in Fig. 8). Common Pb reported by these authors for the Saganaga pluton (SA, Fig. 8) has a more radiogenic composition than IC, but a projection of these values along a 2680 Ma isochron points to an initial Pb composition similar to that of the Icarus pluton. The Pb isotopic composition measured in this study for leached feldspar of sample Pg (footnote to Table 1) yields a composition closer to that of the Burchell Lake pluton (Corfu and Stott, 1986; BP in Fig. 8), but it leads to corrected titanite ages that are marginally older than the zircon age, suggesting either isotopic disequilibrium between titanite and feldspar or the presence of some inherited titanite cores. Initial Pb for samples Ke and Pm was corrected using an arbitrary value intermediate between those of Icarus and Burchell Lake, with an uncertainty encompassing the range between these values.

The zircon population in the Hermia stock sample (He) is dominated by zoned crystals, generally in an advanced state of metamictization. Cores are also zoned (Fig. 3J) and appear to be synmagmatic phases, because a core-bearing grain yields a $^{207}Pb/^{206}Pb$ age similar to that of the general population. The five zircon analyses fit a line forced through about 1000 Ma, implying that the zircons were affected by Keweenawan Pb loss. The line has an upper intercept at 2687 ± 3 Ma, which is a maximum age if one considers that more recent Pb loss may have shifted at least some of the data below the original Pb-loss trajectory (e.g., Corfu and Muir, 1989a). Two analyses carried out on titanite show an uncommonly pronounced discordance of as much as 6.4%. The Pb composition of feldspar in this sample is somewhat radiogenic, but it projects toward the composition of BP (Fig. 8); hence the latter was used to correct initial Pb in titanite, resulting in identical $^{207}Pb/^{206}Pb$ ages of 2678 ± 6 Ma. Rutile occurs in this sample as yellow to orange, generally translucent euhedral prisms with low U contents of 5–7 ppm, and Th/U ratios of 1.1 to 1.2.

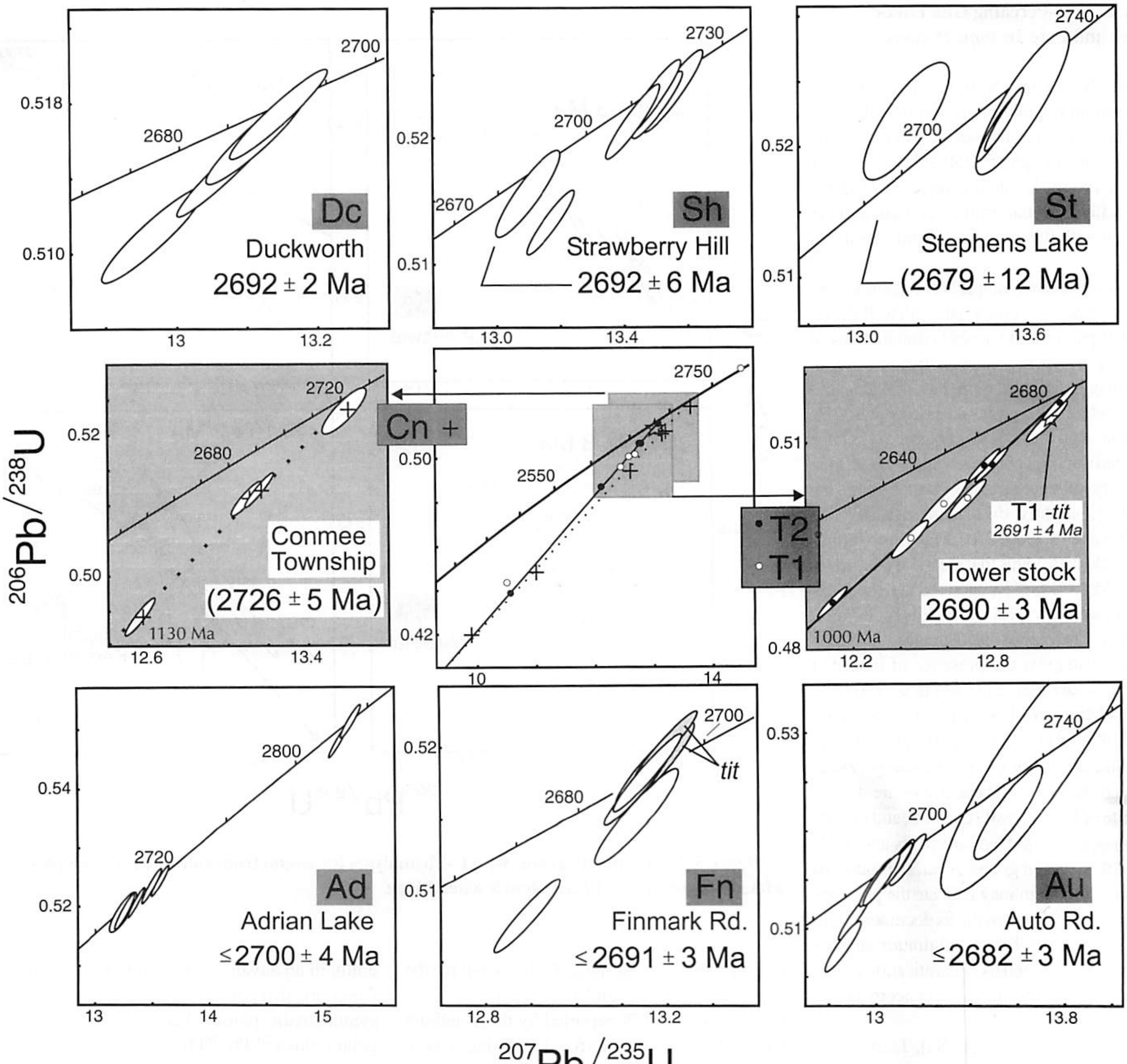


**Figure 6. Concordia diagrams with U-Pb analyses for zircon and titanite from volcanic-sedimentary samples and a syenite stock of the Shebandowan assemblage and from three clastic sedimentary units (Ad, Fn, and Au).**

The high Th/U ratios are similar to those in zircon (0.7–1.2) and lower than in titanite (>7.1) and contrast with the generally very low values observed for rutile. One rutile fraction is 2.1% discordant and overlaps one of the titanite data points while two other rutile fractions are concordant, yielding $^{207}Pb/^{206}Pb$ ages of 2690 ± 9 and 2688 ± 7 Ma. The complex U-Pb pattern for this sample prevents the derivation of a precise and reliable age: use of all the analyses and the error expansion procedure of Davis (1982) provides our best estimate of 2684 +6/–4 Ma (Fig. 7).

## DISCUSSION

The U-Pb ages of the Shebandowan greenstone belt define a relatively simple sequence of events marked by magmatism at and perhaps before 2750 Ma in the Northern Light Gneiss, main-stage development of a volcanic terrain at about 2720 Ma, renewed volcanic and plutonic activity at 2695 Ma, probably during compression, deposition of the Shebandowan assemblage and alkalic to tonalitic plutonism at about 2690 Ma, and finally plutonism, deposition of the late tectonic Auto Road assemblage and transpressive deformation at 2684 to 2680 Ma (Fig. 9).

### Early Magmatism

The available data suggest that the Shebandowan greenstone belt contains only small amounts of pre-2720 Ma crust. One sample from the Northern Light Gneiss indicates an age of 2750 Ma, whereas a second gneiss sample suggests formation of tonalite at about 2710–2690

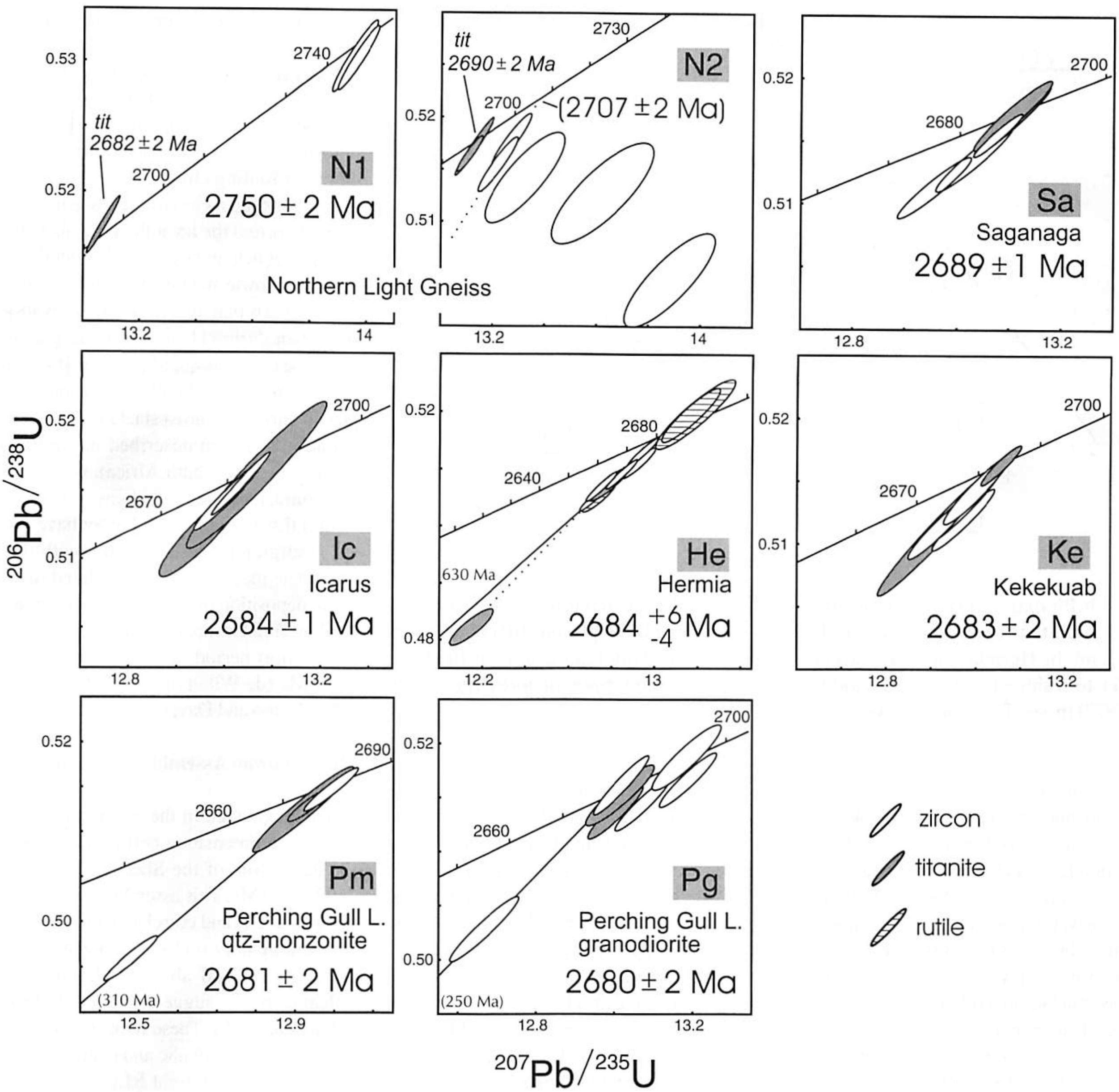


**Figure 7. Concordia diagrams with U-Pb analyses for zircon, titanite, and rutile from the Northern Light Gneiss and syntectonic to late tectonic plutons.**

Ma, later than the Greenwater assemblage. The earlier U-Pb data by Hart and Davis (1969) and the Rb-Sr data of Hanson et al. (1971) also indicated formation of the gneisses at about 2700 Ma. Indirect evidence for a post-Greenwater age of much tonalite also includes the observation that the gneisses locally cut or include xenoliths of greenstone assemblages (Percival and Stern, 1984). Older apparent ages are observed only for xenocrystic or detrital zircons in samples N2 ([?]>2765 and 2823 Ma), Ks (2766 Ma), Po (2761 Ma), T1 (2780 Ma) and the two grains coinciding at 2830 Ma in Ad.

**Greenwater Assemblage**

The 2722–2718 Ma Greenwater assemblage is the product of the dominant volcanic episode in the development of the greenstone belt. Geochemical data for the mafic and ultramafic rocks show a wide compositional spectrum from komatiite, to komatiitic basalts, high Fe- and high Mg tholeiites, and calc-alkalic basalts. The rare earth element (REE) data of the basalts display generally flat patterns or show slight light REE enrichment and abundances varying from 10–40 × chondrite (Brown, 1995; Rogers and Berger, 1995; Osmani, 1996, 1997). Intermediate and felsic volcanic rocks are dominantly calc-alkalic and show moderately fractionated REE patterns. Some exceptions include a felsic volcanic complex (Amp Lake) north of Middle Shebandowan Lake (Fig. 2), which has flat REE patterns at 20–30 × chondrite and significant Eu anomalies, suggesting a control by low-pressure fractionation of basalt. Ultramafic to mafic intrusive rocks show mainly flat REE patterns, at 1 to 10 × chondrite, with moderate light REE fractionation in some samples. Positive Eu anomalies are observed in anorthosites (Osmani, 1996, 1997). This geo-

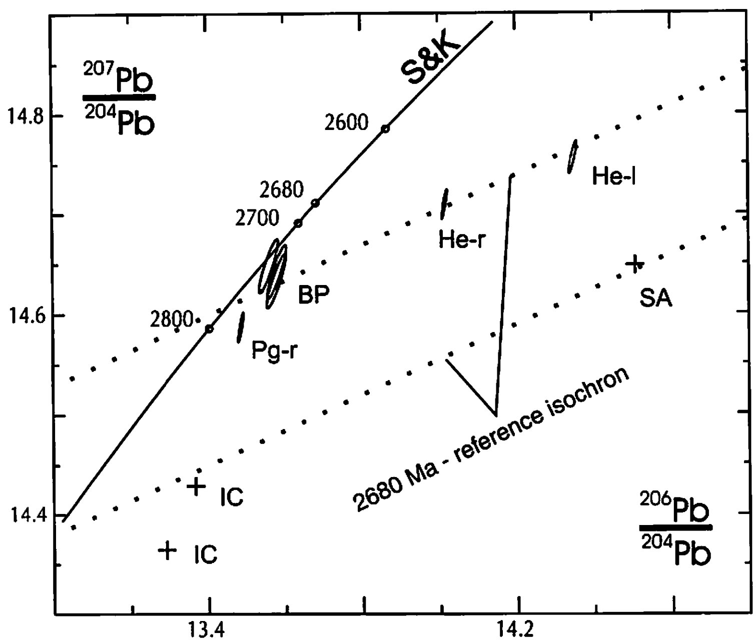


**Figure 8. Pb-Pb diagram showing Pb compositions for feldspar from the Icarus (IC) and Saganaga (SA) plutons (Arth and Hanson, 1975), the Burchell Lake pluton (BP) (Corfu and Stott, 1986), and the Hermia stock (He-r and He-l) and Perching Gull Lake granodiorite (Pg-r) (r and l refer to residue from leaching and leachate, respectively). S&K denotes Stacey and Kramers (1975) model Pb growth curve.**

chemical variation, together with the coeval occurrence of komatiites, basalts, calc-alkalic flows, pyroclastics, and layered peridotite-gabbro-anorthosite complexes, is broadly comparable to the relations observed in the 2700 Ma Bourlamaque–Blake River–Kinojevis–Montcalm magmatic system of the Abitibi greenstone belt. The analogy, therefore, suggests a genesis of the Greenwater assemblage in a rifted active arc, or a coupled arc-backarc system analogous to the settings postulated for the southern Abitibi greenstone belt (e.g., Jackson et al., 1994).

**Kashabowie Assemblage**

The Kashabowie assemblage postdates development of the Greenwater volcanic complex by a period of more than 20 m.y., during which time little or no magmatic activity is recorded in the area. The Kashabowie assemblage is correlative with the previously dated 2696 ± 2 Ma Shebandowan pluton (Corfu and Stott, 1986), which was emplaced during or following $D_1$ deformation. The Kashabowie felsic volcanic rocks are of calc-alkalic affinity and have monotonously fractionated REE patterns comparable to those of porphyry dikes and sills and of tonalite in the Shebandowan pluton (Osmani, 1996). The fragmental and tuffaceous samples Ks and Bu contain abundant xenocrystic zircons, but the youngest grains in both samples and all four grains in the fine-grained tuff (Mb) at Mabella coincide at 2696 to 2694 Ma and are identical to the age of the Shebandowan pluton. Although these 2696–2694 Ma zircon grains could be xenocrystic, there are arguments suggesting that they probably date extrusion of the pyroclastic rocks. One of the arguments supporting a pre-Shebandowan assemblage age is the petrographic and compositional distinction of these volcanic units, notably a lack of hornblende-phyric and alkalic rocks characteristic of the Timiskaming-type succession in the area. Whereas the Shebandowan assemblage rocks appear to form mainly a thin cover on the underlying successions, the Kashabowie assemblage units are interlayered (at map scale) with volcanic and mafic-ultramafic intrusive rocks characteristic of the Greenwater assemblage (Fig. 2). These relationships suggest that the Kashabowie assemblage was erupted and tectonically interleaved ($D_1$) with thrust panels of Greenwater assemblage rocks during a relatively short time span preceding the development of the Shebandowan assemblage.

The Shebandowan pluton and Kashabowie assemblage are coeval with 2696 Ma tonalitic dikes intruded into metasedimentary units of the Quetico Subprovince to the north (Davis, 1996). Deposition of the Quetico sediments occurred immediately prior to these events, as evidenced by the occurrence of detrital zircons as young as 2699 Ma. Quetico sedimentation reflects erosion caused by uplift during large-scale collisional orogeny (Davis et al., 1990; Davis, 1996).

In the boundary zone between the Vermilion belt and the Quetico Subprovince (Fig. 1), the $D_1$ deformation event produced thrusting and recumbent folding (Bauer et al., 1992). The inferred stacking of Greenwater assemblage cyclical units across the breadth of the Shebandowan greenstone belt and the complex interleaving of the Kashabowie and Greenwater assemblages in the northern part of the Shebandowan greenstone belt during $D_1$ were probably a result of the same compressional process. It is conceivable that the 2695 Ma felsic intrusions were emplaced during $D_1$ thrust stacking. A very similar situation has been described in the Barberton greenstone belt (South Africa), where shallow-level intrusions and felsic domes were emplaced within thrust zones, which may have repeated the stratigraphy. At Barberton, both thrusting and felsic magmatism were related to synorogenic deposition of clastic sedimentary rocks of the Fig Tree Group, the whole spanning a relatively short period of time between 3230 and 3215 Ma (de Wit et al., 1987; de Ronde et al., 1991; Kamo and Davis, 1994).

**Shebandowan Assemblage–Saganaga pluton**

The next stage in the evolution of the Shebandowan greenstone belt is characterized by the deposition of the Shebandowan Group at 2692–2689 Ma. This assemblage is composed of volcanic rocks and correlative clastic and chemical sedimentary rocks. The brecciated scoriaceous aspect and absence of pillows of the volcanic rocks suggest subaerial deposition (Thurston, 1985). These rocks range from calc-alkalic to locally alkalic and exhibit fractionated REE patterns with light REE varying between about 10 and 100× chondrite (Stern, 1984; Brown, 1995; Rogers and Berger, 1995; Carter, 1993). Similar patterns also characterize the coeval syenitic to dioritic Tower stock (light REE = 200–400; Carter, 1993) and the tonalitic Saganaga pluton (light REE = 20–40; Evans and Hanson, 1993). The sedimentary rocks include iron formation, chert, and clastic rocks ranging from mudstone to conglomerate. In northern parts of the Shebandowan greenstone belt the sedimentary environment appears to have been shallow marine to subaerial (Shegelski, 1980). The turbidite sequence in Adrian Township, however, indicates deep-water sedimentation (Rogers and Berger, 1995). Unfortunately, the detrital zircon data do not conclusively prove a Shebandowan assemblage age for these turbidites, and it is possible that they may have

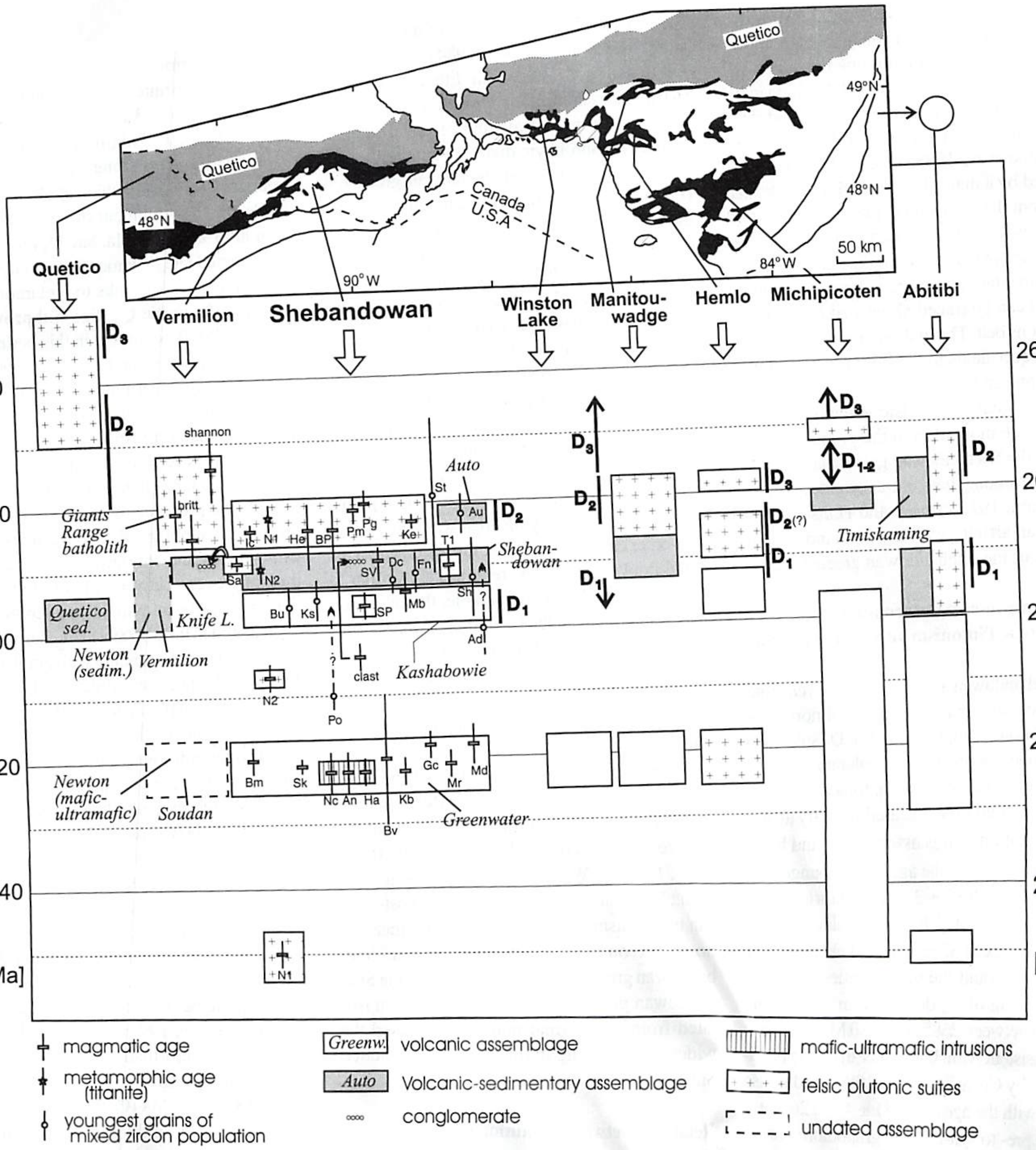


**Figure 9. Schematic diagram summarizing the main stages of greenstone belt construction and Kenoran deformation in the Shebandowan greenstone belt and regional correlations. The plotted ages are from this paper, Corfu and Stott (1986), and Boerboom and Zartman (1993). References for the other areas are quoted in the text. An exact correlation of structural phases between different areas is hampered in part by uncertainties regarding the timing, nature, and diachroneity of deformation events.**

been deposited during Quetico or Kashabowie assemblage formation.

The Shebandowan assemblage is very similar in terms of lithology and geochemistry to the classical Timiskaming assemblage in the southern Abitibi greenstone belt (Cooke and Moorhouse, 1969), but it has a different geometry. In the Abitibi greenstone belt the Timiskaming assemblage is enclosed largely within deep tectonic wedges with few occurrences located within shallow, fault-bounded depressions. By contrast, the Shebandowan assemblage in the Shebandowan greenstone belt appears to form a relatively thin layer on top of the underlying older units. The similarity between the two assemblages likely reflects comparable magmatic geneses and depositional environments, whereas the different modes of preservation reflect the local effects of late Archean tectonism.

The Saganaga pluton shed detritus to form the sedimentary rocks of the Knife Lake Group (Goldich et al., 1972), hence deposition is constrained at ≤2689 Ma (Fig. 9). The Knife Lake

Group may be correlative with the Vermilion Formation, a succession of *turbidites* and reworked tuffs overlying dominantly mafic volcanic units and iron formation of the Soudan belt (Morey, 1980; Jirsa et al., 1992). The Soudan belt is characterized by large-scale fold structures (Hudleston et al., 1988; Jirsa et al., 1992) and is separated by a major fault, the Mud Creek shear zone, from the homoclinal, predominantly north facing Newton belt to the north. The Newton belt s composed of mafic-ultramafic units in the west nd sedimentary and felsic volcanic units in the ast, and can be traced along strike toward the aganagons belt. The mafic-ultramafic units may ell be equivalents to the lithologically similar ıganagons and Greenwater assemblages. The etasedimentary and felsic volcanic member, wever, are more akin to the younger assemges of the Shebandowan greenstone belt. The currence among them of trachyandesites (Arth l Hanson, 1975; Shirey and Hanson, 1984) gests an affinity with the Shebandowan asıblage of the Shebandowan greenstone belt.

## n Transpressive Deformation, Tectonic Plutonism and Sedimentation

ıe Shebandowan assemblage was overprinted structures formed as a result of northwested oblique compression. The $D_2$ structures, include a dominantly east plunging mineral on, local folds, and a steep foliation, are also t in the Auto Road metasedimentary assem- Deposition of this assemblage, and hence constrained by the age of the youngest deircons at ≤2682 ± 3 Ma. $D_2$ fabrics, howvere overprinted by the emplacement of such as the 2683 ± 3 Ma Kekekuab pluton. into account the uncertainties on theses ıe timing of $D_2$ deformation is therefore ined between 2685 and 2680 Ma. This time consistent with, but tighter than, the previ-ket by Corfu and Stott (1986), and is also nt with the ages of 2681 ± 4 and 2685 ± 4 he pre- to syn-$D_2$ Britt granodiorite in the Range batholith to the west (Boerboom and ı, 1993).

ate tectonic plutons display a range of itions from tonalite, present locally in the Lake pluton, through monzodiorite, granquartz monzonite and syenite, to the late phases surrounding the Perching Gull uton. The available geochemistry shows late plutons are genetically similar to the ns associated with the Shebandowan ase. In general, all these rocks exhibit steep terns with light REE levels varying from 0 × chondritic (Arth and Hanson, 1975; 984; Carter, 1993; Evans and Hanson, s discussed in detail by Stern (1984) and Stern et al. (1989), the genesis of this sanukitoid suite (Shirey and Hanson, 1984) is attributed to fractionation of large ion lithophile element (LILE)–enriched monzodioritic parental melts produced by partial melting of metasomatized mantle. Lamprophyre dikes are another late tectonic element of the Shebandowan greenstone belt, displaying characteristics broadly similar to the sanukitoid suite (Wyman and Kerrich, 1989) and likely reflecting a cogenetic origin. The 2680 Ma granite-granodiorite suite cutting the Perching Gull Lake pluton has more evolved geochemical features, and was discussed by Stern (1984) in terms of derivation from partial melting of tonalitic crust. A crustal origin of the granite or widespread contamination of the original magma is supported by the presence of abundant xenocrystic zircons in the granodiorite (Pg). The granite intrudes the quartz monzonite, but it yields essentially the same age, suggesting that partial melting of the underlying crust was a local, second-order effect caused by the emplacement of the sanukitoid magmas. The relations are similar to those observed for a comparable, though older, late tectonic suite in the Uchi Subprovince (Corfu and Stott, 1993). A probable origin by partial melting of graywackes has been proposed for the 2674 ± 5 Ma Shannon Lake granite, the youngest S-type granite in the Giants Range batholith (Boerboom and Zartman, 1993).

Younger ages between about 2670 and 2650 Ma record the development of extensive migmatites and granites in the core of the Quetico Subprovince (Percival and Sullivan, 1988; Bauer et al., 1992; D. W. Davis, 1996, personal commun.; Pan et al., 1998). The extensive post-2680 Ma magmatism in the Quetico Subprovince had no effect on titanites or rutile of the Shebandowan greenstone belt, showing that the Shebandowan greenstone belt must have been isolated from the thermal plume that caused the widespread melting in the core of the Quetico Subprovince.

## Relations Between Evolution of Shebandowan Greenstone Belt and the Central–Eastern Wawa Subprovince

There are similarities between the evolution of the Shebandowan greenstone belt and the Manitouwadge and Winston Lake greenstone bels hosting volcanogenic massive sulfide deposits in the eastern Wawa Subprovince (Fig. 9).All three areas underwent the same stage of mafic to felsic volcanism at 2720 Ma (Davis et a., 1994; Zaleski et al., 1995), suggesting that they were originally part of the same active arc-backarc system. Moreover, at Manitouwadge, a first $D_1$ deformation event was apparently related to thrusting and was followed by the deposition of graywackes at or after 2692 ± 1 Ma $D_2$ deformation, causing widespread isoclina folding, overprinted a suite of plutons with age between 2687 ± 3 and 2680 ± 3 Ma (Zalesk et al., 1995). The main difference to the Shebandowan greenstone belt concerns the youngest tectonism, which at Manitouwadge includes the development of large scale $D_3$ folds at or after 2677 ± 2 Ma, late $D_4$ kink bands, and a protracted late metamorphic and hydrothermal evolution showing links to metamorphism and magmatism in the Quetico Subprovince (Pan et al., 1998). By contrast, in this period the Shebandowan greenstone belt underwent only minor deformation forming conjugate kink bands and remained screened from the effects of Quetico metamorphism.

Similarities between the Shebandowan greenstone belt and the Hemlo greenstone belt (Fig. 9) include the presence of ca. 2719 Ma magmatic rocks, an assemblage of 2695 Ma pyroclastic volcanic rocks, the inferred occurrence of a $D_1$ thrusting event between about 2695 and 2688 Ma, and significant plutonism at 2688–2684 Ma (Corfu and Muir, 1989a). $D_2$ deformation at Hemlo appears to correlate with emplacement of the 2688 Ma magmatic suite, but the indications remain somewhat conflicting (Corfu and Muir, 1989a). The late evolution at Hemlo is closer to that of Manitouwadge with $D_3$ broadly synchronous with a late plutonic phase at 2678 Ma, followed by a succession of hydrothermal events as late as 2630 Ma (Corfu and Muir, 1989b).

In the Michipicoten belt of the eastern Wawa Subprovince, clastic sedimentary rocks yielding depositional ages of ≤2682 Ma—similar to the Auto Road assemblage of the Shebandowan greenstone belt—underwent complex deformation including recumbent folding, imbrication, and refolding between ≤2682 Ma and 2671 Ma (Corfu and Sage, 1992; Arias and Helmstaedt, 1990). Major deformation also overprinted the Timiskaming assemblage of the Abitibi belt after about 2680–2677 Ma (Corfu et al., 1991), later than the corresponding phase in the Shebandowan greenstone belt.

## CONCLUSIONS

The U-Pb results establish the following main events for the evolution of the Shebandowan greenstone belt.

1. A major volcanic-plutonic complex developed, probably in an arc-backarc setting at about 2720 Ma.

2. A second episode of magmatism occurred at about 2695 Ma, producing tonalites, porphyries and pyroclastic volcanic rocks.

3. There was $D_1$ deformation and thrust imbrication of 2720 and 2695 Ma volcanic units at

the northern edge of the Shebandowan greenstone belt.

4. Eruption of calc-alkalic to alkalic volcanic rocks was accompanied by intrusion of tonalitic and syenitic plutons, and was coeval with the deposition of unconformable subaerial to shallow-water sedimentary rocks in northern parts of the belt and of deep-water turbidites in southern and western domains at about 2690 Ma.

5. Intrusion of a younger suite of sanukitoid plutons and late clastic sedimentation occurred between about 2685 and 2680 Ma, in connection with deformation ($D_2$) caused by oblique northwest-directed compression.

Although the data document the presence of a 2750 Ma tonalitic phase in the Northern Light Gneiss Complex, the bulk of the region appears to have formed mainly by juvenile accretion in an oceanic marginal basin. The 2720 Ma volcanic-plutonic assemblage is correlative with volcanic assemblages hosting volcanogenic massive sulfide-deposits at Winston Lake and Manitouwadge, and they share a very similar tectonic and magmatic evolution. Only the late evolution is distinct: the Shebandowan greenstone belt became a quiescent high crustal-level terrain while the Winston Lake and Manitouwadge greenstone belts, and to some degree the Hemlo greenstone belt, became involved in the extensive post-2680 Ma tectonism and metamorphism that dramatically affected the Quetico Subprovince.

The late Archean evolution of the Shebandowan greenstone belt fits current actualistic models, whereby the greenstone belt was accreted as a consequence of magmatic and tectonic processes in a subduction setting concluded by the Superior Province–wide compressional orogeny. The late history of $D_2$ compression and plutonism postdates the comparable late-stage history of the Uchi Subprovince in the northern Superior Province, which culminated by 2698 Ma (Corfu and Stott, 1993). The geochronological constraints on the late tectonic history of these subprovinces are strong supporting evidence for growth of the Superior Province by a progressive southward accretion of superterranes (Stott et al., 1987).

## ACKNOWLEDGMENTS

The study was carried out at the Jack Satterly Laboratory of the Royal Ontario Museum as a part of a geochronological program supported by the Ontario Geological Survey. We benefited from advice in sampling and discussions with M. Carter, I. Osmani, B. Berger, H. Brown, C. Farrow, and Ph. Fralick. We thank R. Tahiste for performing most of the sample preparation and for help with the chemical procedures and mass spectrometry, and the Jack Satterly staff for general assistance. P. Thurston, Z. Peterman and P. K. Sims provided helpful comments and reviews. The paper is published with permission of the Ontario Geological Survey.

## REFERENCES CITED

Arias, Z. G., and Helmstaedt, H., 1990, Structural evolution of the Michipicoten (Wawa) greenstone belt, Superior Province: Evidence for an Archean fold and thrust belt, *in* Milne, V. G., ed., Geoscience research grant program, summary of research 1989–1990: Ontario Geological Survey Miscellaneous Paper 150, p. 107–114.

Arth, J. G., and Hanson, G. N., 1975, Geochemistry and origin of the early Precambrian crust of northeastern Minnesota: Geochimica et Cosmochimica Acta, v. 39, p. 325–362.

Bauer, R. L., Hudleston, P. J., and Southwick, D. L., 1992, Deformation across the western Quetico subprovince and adjacent boundary regions in Minnesota: Canadian Journal of Earth Sciences, v. 29, p. 2087–2103.

Boerboom, T. J., and Zartman, R. E., 1993, Geology, geochemistry, and geochronology of the central Giants Range batholith, northeastern Minnesota: Canadian Journal of Earth Sciences, v. 30, p. 2510–2522.

Borradaile, G., and Brown, H., 1987, The Shebandowan Group: "Timiskaming-like" Archean rocks in northwestern Ontario: Canadian Journal of Earth Sciences, v. 24, p. 185–188.

Borradaile, G., and Spark, R., 1991, Deformation of the Archean Quetico-Shebandowan subprovince boundary in the Canadian Shield near Kashabowie, northern Ontario: Canadian Journal of Earth Sciences, v. 28, p. 116–125.

Brown, G. H., 1995, Precambrian geology, Oliver and Ware townships: Ontario Geological Survey Report 294, 48 p.

Carter, M. W., 1985, Forbes and Conmee Townships, District of Thunder Bay, *in* Wood, J., White, O. L., Barlow, R. B., and Colvine, A. C., eds., Summary of field work and other activities 1985: Ontario Geological Survey Miscellaneous Paper 126, p. 60–65.

Carter, M. W., 1986, Blackwell and Laurie Townships, District of Thunder Bay, *in* Thurston, P. C., White, O. L., Barlow, R. B., Cherry, M. E., and Colvine, A. C., eds., Summary of field work and other activities 1986: Ontario Geological Survey Miscellaneous Paper 132, p. 85–89.

Carter, M. W., 1987, Alkalic rocks of the Thunder Bay area, *in* Barlow, R. B., Cherry, M. E., Colvine, A. C., Dressler, B. O., and White, O. L., eds., Summary of field work and other activities 1987: Ontario Geological Survey Miscellaneous Paper 137, p. 108–115.

Carter, M. W., 1992, Geology and mineral potential of the Tower syenite stock, Conmee Township, District of Thunder Bay, *in* Dressler, B. O., Baker, C. L., and Blackwell, B., eds., Summary of field work and other activities 1992: Ontario Geological Survey Miscellaneous Paper 160, p. 60–63.

Carter, M. W., 1993, The geochemical characteristics of Neoarchean alkalic magmatism in central Superior Province, Ontario, *in* Baker, C. L., Dressler, B. O., deSouza, H. A. F., Fenwick, K. G., Newsome, J. W., and Owsiaki, L., eds., Summary of field work and other activities 1993: Ontario Geological Survey Miscellaneous Paper 162, p. 13–19.

Catanzaro, E. J., and Hanson, G. N., 1971, U-Pb ages for sphene from early Precambrian igneous rocks in northeastern Minnesota–northwestern Ontario: Canadian Journal of Earth Sciences, v. 8, p. 1319–1324.

Chorlton, L., 1985, Geological setting of gold mineralization in central Moss Township, Shebandowan greenstone belt, northwestern Ontario, *in* Wood, J., White, O. L., Barlow, R. B., and Colvine, A. C., eds., Summary of field work and other activities 1985: Ontario Geological Survey Miscellaneous Paper 126, p. 215–221.

Chorlton, L. B., 1987, Geological setting of gold mineralization in the western part of the Shebandowan greenstone belt, District of Thunder Bay, northwestern Ontario: Ontario Geological Survey Open-File Report 5636, 348 p.

Cooke, D. L., and Moorhouse, W. W., 1969, Timiskaming volcanism in the Kirkland Lake area, Ontario, Canada: Canadian Journal of Earth Sciences, v. 6, p. 117–132.

Corfu, F., and Muir, T. L., 1989a, The Hemlo–Heron Bay greenstone belt and Hemlo Au-Mo deposit, Superior Province: I. Sequence of igneous activity determined by zircon U-Pb geochronology: Chemical Geology (Isotope Geoscience Section) v. 79, p. 183–200.

Corfu, F., and Muir, T. L., 1989b, The Hemlo–Heron Bay greenstone belt and Hemlo Au–Mo deposit, Superior Province: II. Timing of metamorphism, alteration and Au mineralization from titanite, rutile, and monazite U-Pb geochronology: Chemical Geology (Isotope Geoscience Section), v. 79, p. 201–223.

Corfu, F., and Noble, S. R., 1992, Genesis of the southern Abitibi greenstone belt, Superior Province, Canada: Evidence from zircon Hf-isotope analyses using a single filament technique: Geochimica et Cosmochimica Acta, v. 56, p. 2081–2097.

Corfu, F., and Sage, R. P., 1992, U-Pb age constraints for deposition of clastic metasedimentary rocks and late-tectonic plutonism, Michipicoten Belt, Superior Province: Canadian Journal of Earth Sciences, v. 29, p. 1640–1651.

Corfu, F., and Stott, G. M., 1986, U-Pb ages for late magmatism and regional deformation in the Shebandowan Belt, Superior Province, Canada: Canadian Journal of Earth Sciences, v. 23, p. 1075–1082.

Corfu, F., and Stott, G. M., 1993, Age and petrogenesis of two late Archean magmatic suites, northwestern Superior Province, Canada: Zircon U-Pb and Lu-Hf isotopic relations: Journal of Petrology, v. 34, p. 817–838.

Corfu, F., Jackson, S. L., and Sutcliffe, R. H., 1991, U-Pb ages and tectonic significance of late alkalic magmatism and nonmarine sedimentation: Timiskaming Group, southern Abitibi belt, Ontario: Canadian Journal of Earth Sciences, v. 28, p. 489–503.

Davidson, D. M., 1980, Emplacement and deformation of the Archean Saganaga batholith, Vermilion District, northeastern Minnesota: Tectonophysics, v. 66, p. 179–195.

Davis, D. W., 1982, Optimum linear regression and error estimation applied to U-Pb data: Canadian Journal of Earth Sciences, v. 19, p. 2141–2149.

Davis, D. W., 1996, U-Pb age patterns for detrital zircons from the western Superior Province: Witnesses to orogeny: Geological Association of Canada–Mineralogical Association of Canada, Annual Meeting, Winnipeg, Program with Abstracts, v. 21, p. A-21.

Davis, D. W., Pezzutto, F., and Ojakangas, R. W., 1990, The age and provenance of metasedimentary rocks in the Quetico Subprovince, Ontario, from single zircon analyses: Implications for sedimentation and tectonics in the Superior Province: Earth and Planetary Science Letters, v. 99, p. 195–205.

Davis, D. W., Schandl, E. S., and Wasteneys, H. A., 1994, U-Pb dating of minerals in alteration haloes in Superior province massive sulfide deposits: Syngenesis versus metamorphism: Contributions to Mineralogy and Petrology, v. 115, p. 427–437.

de Ronde, C. E. J., Kamo, S., Davis, D. W., de Wit, M. J., and Spooner, E. T. C., 1991, Field, geochemical and U-Pb isotopic constraints from hypabyssal felsic intrusions within the Barberton greenstone belt, South Africa: Implications for tectonics and the timing of gold mineralization: Precambrian Research, v. 49, p. 261–280.

de Wit, M. J., Armstrong, R., Hart, R. J., and Wilson, A. H., 1987, Felsic igneous rocks within the 3.3 to 3.5 Ga Barberton greenstone belt: High crustal level equivalents of the surrounding tonalite-trondhjemite terrain, emplaced during thrusting: Tectonics, v. 6, p. 529–549.

Evans, O. C., and Hanson, G. N., 1993, Accessory-mineral fractionation of rare-earth element (REE) abundances in granitoid rocks: Chemical Geology, v. 110, p. 69–93.

Farrow, C. E. G., 1993, Base metal sulphide mineralization, Shebandowan greenstone belt, *in* Baker, C. L., Dressler, B. O., deSouza, H. A. F., Fenwick, K. G., Newsome, J. W., and Owsiaki, L., eds., Summary of field work and other activities 1993: Ontario Geological Survey Miscellaneous Paper 162, p. 87–96.

Farrow, C. E. G., 1995, Alteration and sulphide mineralogy associated with base metal mineralization, Shebandowan greenstone belt, *in* Ayer, J. A., and 11 others, eds., Summary of field work and other activities 1995: Ontario Geological Survey Miscellaneous Paper 164, p. 82–86.

Goldich, S. S., Hanson, G. N., Hallford, C. R., and Mudrey, M. G., 1972, Early Precambrian rocks in the Saganaga Lake–Northern Light Lake area, Minnesota-Ontario. Part I. Petrology and structure, *in* Doe, B. R., and Smith, D. K., [illegible]es in mineralogy and Precambrian geology: G[illegible] Society of America Memoir 135, p. 151–178.

Grout, F. [illegible]29, The Saganaga granite of Minnesota-Ontario: Journ[illegible] of Geology, v. 37, p. 562–591.

Hanson, G. N., and Goldich, S. S., 1972, Early Precambrian rocks in the Saganaga Lake–Northern Light Lake area, Minnesota-Ontario. Part II. Petrogenesis, *in* Doe, B. R., and Smith, D. K., eds., Studies in mineralogy and Precambrian geology: Geological Society of America Memoir 135, p. 179–192.

Hanson, G. N., Goldich, S. S., Arth, J. G., and Yardley, D. H., 1971, Age of the early Precambrian rocks of the Saganaga Lake–Northern Light Lake area, Ontario-Minnesota: Canadian Journal of Earth Sciences, v. 8, p. 1110–1124.

Harris, F. R., 1968, Geology of the Saganagons area: Ontario Department of Mines Geological Report 66, 30 p.

Hart, S. R., and Davis, G. L., 1969, Zircon U-Pb and whole-rock Rb-Sr ages and early crustal development near Rainy Lake, Ontario: Geological Society of America Bulletin, v. 80, p. 595–616.

Hudleston, P. J., Schultz-Ela, D., and Southwick, D. L., 1988, Transpression in an Archean greenstone belt, northern Minnesota: Canadian Journal of Earth Sciences, v. 25, p. 1060–1068.

Jackson, S. L., Fyon, J. A., and Corfu, F., 1994, Review of Archean supracrustal assemblages of the southern Abitibi greenstone belt in Ontario, Canada: Products of microplate interaction within a large-scale plate-tectonic setting: Precambrian Research, v. 65, p. 183–205.

Jaffey, A. H., Flynn, K. F., Glendenin, L. E., Bentley, W. C., and Essling, A. M., 1971, Precision measurement of half-lives and specific activities of $^{235}U$ and $^{238}U$: Physical Review C: Nuclear Physics, v. 4, p. 1889–1906.

Jirsa, M. A., Southwick, D. L., and Boerboom, T. J., 1992, Structural evolution of Archean rocks in the western Wawa subprovince, Minnesota: Refolding of precleavage nappes during $D_2$ transpression: Canadian Journal of Earth Sciences, v. 29, p. 2146–2155.

Kamo, S. L., and Davis, D. W., 1994, Reassessment of Archean crustal development in the Barberton Mountain Land, South Africa, based on U-Pb dating: Tectonics, v. 13, p. 167–192.

Krogh, T. E., 1973, A low contamination method for hydrothermal decomposition of zircon and extraction of U-Pb for isotopic age determinations: Geochimica et Cosmochimica Acta, v. 37, p. 485–494.

Krogh, T. E., 1982, Improved accuracy of U-Pb zircon ages by the creation of more concordant systems using an air abrasion technique: Geochimica et Cosmochimica Acta, v. 46, p. 637–649.

Morey, G. B., 1980, A brief review of the geology of the western Vermilion district, northeastern Minnesota: Precambrian Research, v. 11, p. 247–265.

Mortensen, J. K., Roddick, J. C., and Parrish, R. R., 1992, Evidence for high levels of unsupported radiogenic $^{207}Pb$ in zircon from a granitic pegmatite: Implications for interpretation of discordant U-Pb data [abs.]: Eos (Transactions, American Geophysical Union), v. 73, p. 370.:

Osmani, I. A., 1996, Geology and mineral potential of the upper and middle Shebandowan Lakes area, west-central Shebandowan greenstone belt: Ontario Geological Survey, Open File Report 5938, 82 p.

Osmani, I. A., 1997, Geology and mineral potential: Greenwater Lake area, west-central Shebandowan greenstone belt: Ontario Geological Survey Report 296, 135 p.

Osmani, I. A., and Payne, J., 1993, Geology of Begin, Lamport and parts of Haines and Hagey Townships, District of Thunder Bay, *in* Baker, C. L., Dressler, B. O., deSouza, H. A. F., Fenwick, K. G., Newsome, J. W., and Owsiaki, L., eds., Summary of field work and other activities 1993: Ontario Geological Survey Miscellaneous Paper 162, p. 237–242.

Osmani, I. A., Payne, J., and Lavigne, M. J., 1992, Geology of the western Greenwater Lake area, District of Thunder Bay, Ontario, *in* Dressler, B. O., Baker, C. L., and Blackwell, B., eds., Summary of field work and other activities 1992: Ontario Geological Survey Miscellaneous Paper 160, p. 218–227.

Pan, Y., Fleet, M. E., and Heaman, L., 1998, U-Pb geochronological constraints on the Quetico granulite zone of the Superior Province, Canada: Precambrian Research (in press).

Percival, J. A., 1983, Preliminary results of geological synthesis in the western Superior Province, *in* Current research, Part A: Geological Survey of Canada Paper 83–1A, p. 125–131.

Percival, J. A., and Stern, R. A., 1984, Geological synthesis in the western Superior Province, Ontario, *in* Current research, Part A: Geological Survey of Canada Paper 84–1A, p. 397–408.

Percival, J. A., and Sullivan, R. W., 1988, Age constraints on the evolution of the Quetico Belt, Superior Province, Canada, *in* Current research: Geological Survey of Canada Paper 88–2, p. 97–108.

Percival, J. A., Stern, R. A., and Digel, M. R., 1985, Regional geological synthesis of western Superior Province, Ontario, *in* Current research, Part A: Geological Survey of Canada Paper 85-1A, p. 385–397.

Rogers, M. C., and Berger, B. R., 1995, Precambrian geology, Adrian, Marks, Sackville, Aldina and Duckworth townships: Ontario Geological Survey Report 295, 66 p.

Shegelski, R. J., 1980, Archean cratonization, emergence and red bed development, Lake Shebandowan area, Canada: Precambrian Research, v. 12, p. 331–347.

Shirey, S. B., and Hanson, G. N., 1984, Mantle derived Archean monzodiorites and trachyandesites: Nature, v. 310, p. 222–224.

Stacey, J. S., and Kramers, J. D., 1975, Approximation of terrestrial lead isotope evolution by a two-stage model: Earth and Planetary Science Letters, v. 34, p. 207–226.

Stern, R. A., 1984, Geochemistry of Archean granitic rocks in the Perching Gull Lakes area, northwestern Ontario, *in* Current research, Part B: Geological Survey of Canada Paper 84–1B, p. 143–157.

Stern, R. A., Hanson, G. N., and Shirey, S. B., 1989, Petrogenesis of mantle-derived, LILE-enriched Archean monzodiorites and trachyandesites (sanukitoids) in southwestern Superior Province: Canadian Journal of Earth Sciences, v. 26, p. 1688–1712.

Stott, G. M., 1986, A structural analysis of the central part of the Shebandowan greenstone belt and a crescent-shaped granitoid pluton, northwestern Ontario [Ph.D. dissert.]: Toronto, Ontario, University of Toronto, 285 p.

Stott, G. M., and Schnieders, B. R., 1983, Gold mineralization in the Shebandowan belt and its relation to regional deformation patterns, *in* Colvine, A. C., ed., Geology of gold in Ontario: Ontario Geological Survey Miscellaneous Paper 110, p. 181–193.

Stott, G. M., and Schwerdtner, W. M., 1981, A structural analysis of the central part of the Shebandowan metavolcanic-metasedimentary belt: Ontario Geological Survey Open-File Report 5349, 44 p.

Stott, G. M., Sanborn-Barrie, M., and Corfu, F., 1987, Major transpression events recorded across Archean subprovince boundaries in northwestern Ontario: Summer Field Meeting, Yellowknife, N. W. T., Canada: Geological Association of Canada Program with Abstracts, p. 24.

Thurston, P. C., 1985, Atikokan-Lakehead compilation project, *in* Wood, J., White, O. L., Barlow, R. B., and Colvine, A. C., eds., Summary of field work and other activities 1985: Ontario Geological Survey Miscellaneous Paper 126, p. 54–59.

Tilton, G. R., and Grünenfelder, M. H., 1968, Sphene: Uranium-lead ages: Science, v. 159, p. 1458–1461.

Watkinson, D. H., and Irvine, T. N., 1964, Peridotitic intrusions near Quetico and Shebandowan, northwestern Ontario: A contribution to the petrology and geochemistry of ultramafic rocks: Canadian Journal of Earth Sciences, v. 1, p. 63–98.

Williams, H. R., Stott, G. M., Heather, K. B., Muir, T. L., and Sage, R. P., 1991, Wawa Subprovince, *in* Thurston, P. C., Williams, H. R., Sutcliffe, R. H., and Stott, G. M., eds., Geology of Ontario, Part 1: Ontario Geological Survey Special Volume 4, p. 485–539.

Wyman, D. A., and Kerrich, R., 1989, Archean lamprophyre dikes of the Superior Province, Canada: Distribution, petrology and geochemical characteristics: Journal of Geophysical Research, v. 94, no. B4, p. 4667–4696.

Zaleski, E., Peterson, V. L., Lockwood, H., and van Breemen, O., 1995, Geology, structure and age relationships of the Manitouwadge greenstone belt and the Wawa subprovince boundary, northwestern Ontario, *in* Field trip guidebook: Institute on Lake Superior Geology, 41st annual meeting, Proceedings volume 41, Part 2b, 77 p.



Manuscript Received by the Society June 19, 1997
Revised Manuscript Received January 3, 1998
Manuscript Accepted February 8, 1998


Printed in U.S.A.